Antimicrobial Peptide MPX Against Escherichia Coli O157:H7 Infection and Inhibiting inflammation, Enhancing Epithelial Barrier and Promoting Nutrient Absorption in the Intestine

Xue qin Zhao
Henan Institute of Science and Technology
Lei Wang (wlei_007@163.com)
Henan Institute of Science and Technology
Chun ling Zhu
Henan Institute of Science and Technology
Xiao jing Xia
Henan Institute of Science and Technology
Shou ping Zhang
Henan Institute of Science and Technology
Yi min Wang
Henan Institute of Science and Technology
Hui hui Zhang
Henan Institute of Science and Technology
Yan zhao Xu
Henan Institute of Science and Technology
Shi jun Chen
Henan Institute of Science and Technology
Jin qing Jiang
Henan Institute of Science and Technology
Yong hui He
Henan Institute of Science and Technology
Gai ping Zhang
Henan Agricultural University
Yue yu Bai
Henan Institute of Science and Technology
Hanna Fotina
Sumy National Agrarian University: Sums'kij nacional'nij agrarnij universitet
Jian he Hu
Henan Institute of Science and Technology

Research

Keywords: antimicrobial peptide MPX, Escherichia coli O157:H7, inflammation, intestinal barrier, nutrient absorption

Posted Date: November 23rd, 2020

DOI: https://doi.org/10.21203/rs.3.rs-112032/v1

Abstract

Background: *Escherichia coli* can cause intestinal diseases in humans and livestock, destroy the intestinal barrier, exacerbate systemic inflammation, and seriously threaten human health and animal husbandry development. The antimicrobial peptide MPX is extracted from venom and possesses good antibacterial activity against gram-negative bacteria. The aim of this study was to investigate whether MPX could be effective against *E. coli* infection.

Results: In this study, the CCK-8 and lactic dehydrogenase results showed that MPX exhibited no toxicity in IPEC-J2 cells even at a concentration of 128 μg/mL. Furthermore, MPX notably suppressed the levels of IL-2, IL-6, TNF-α, myeloperoxidase and LDH induced by *E. coli* and reduced inflammation by inhibiting the p-p38-, TLR4- and p-p65-dependent pathways. In addition, MPX improved the expression of ZO-1, occludin, and claudin and enhanced the wound healing ability of IPEC-J2 cells. The therapeutic effect of MPX was evaluated in a murine model, and the results showed that MPX could protect mice against lethal infection with *E. coli*, improve the survival rate of the mice, and reduce the colonization of *E. coli* in organs and feces. H&E staining showed that MPX increased the length of villi and reduced the infiltration of inflammatory cells into the jejunum, and the effect of MPX was better than that of enrofloxacin. The SEM and TEM results showed that MPX effectively ameliorated the damage caused by *E. coli* to the jejunum and increased the number and length of microvilli. In addition, real-time PCR revealed that MPX decreased the expression of IL-2, IL-6, and TNF-α in the jejunum and colon. Furthermore, immunohistochemistry and immunofluorescence studies revealed that MPX could reduce the expression of p-p38 and p-p65 in the jejunum, thereby reducing the secretion of inflammatory factors. Moreover, MPX increased the mRNA and protein expression of ZO-1, occludin and MUC2 in the jejunum and colon, improved the function of the intestinal barrier and promoted the absorption of nutrients.

Conclusion: This study suggests that MPX may be an effective therapeutic agent against *E. coli* infection and other intestinal diseases, laying the foundation for the development of new drugs for bacterial infections.

Background

Escherichia coli is a facultative anaerobe present in the gastrointestinal tracts of humans and animals that causes diarrhea disease, enteritis, host intestinal barrier damage and intestinal microecological disorder, which have high mortality rates and result in great losses worldwide [1]. *E. coli* can also induce urinary tract infections and meningitis in neonates and promote cell apoptosis [2]. Although antibiotics are currently effective in treating *E. coli* infections, diseases caused by *E. coli* have high degrees of sequelae, leading to more easily repeated intestinal infections [3]. Antibiotics are the primary treatment for *E. coli* infection in animal production, leading to increased resistance to antibiotics, such as ampicillin, florfenicol, and gentamicin [4]. Thus, there is a dire need to explore new alternatives to antibiotics in order to resist *E. coli* infections.

Due to the alarming increase in pathogen resistance to conventional antibiotics and threats to public health worldwide, exploring new drugs to treat infections with antimicrobial-resistant pathogens is urgently needed [5]. Antimicrobial peptides are a class of small molecular peptides produced by the innate immune system of the body that can resist pathogenic infection. The functions of antimicrobial peptides include antibacterial, antiviral, anti-inflammatory and immune regulatory function [6, 7], and antimicrobial peptides are currently considered the best alternatives to antibiotics. The antimicrobial peptide MPX is extracted from venom, contains both acidic and basic residues, including three basic residues, and possesses a net charge of 4; MPX has good antibacterial activity against gram-positive and gram-negative microorganisms [8]. At present, Henriksen et al found that modulating peptide hydrophobicity by introducing an unnatural amino acid with an octyl side chain via amino acid substitution at positions 1, 8 and 14 could increase the bactericidal potency of the antimicrobial peptide MPX [9]. Our previous laboratory studies showed that MPX had good antimicrobial activities against *A. pleuropneumoniae* infections, reduced the colonization of *A. pleuropneumoniae* in the lungs, alleviated the symptoms of pneumonia and improved the survival rate of mice [10]. However, the effect of MPX against *E. coli* infections and in the regulation of *E. coli*-induced inflammation and intestinal disruption remains unknown.

In this study, the effects of MPX on *E. coli* -induced intestinal inflammation and barrier dysfunction were investigated in vitro and in vivo. In IPEC-J2 cells, the results showed that MPX exhibited no cytotoxicity and reduced the mRNA expression of IL-2, IL-6 and TNF-α by inhibiting the phosphorylation of p38 and p65. In addition, MPX increased the *E. coli*-induced expression of the tight junction proteins ZO-1 and occludin and promoted the healing of damage to intestinal epithelial cells. These results were further confirmed in vivo. The results showed that MPX could protect against lethal infection with *E. coli*, improve the survival rate of mice, alleviate intestinal inflammation in the jejunum and colon by reducing the expression of inflammatory factors, and increase the expression of tight junction proteins and the number of microvilli, thereby improving intestinal barrier function. These findings suggest a promising protective role of MPX in preventing *E. coli* infections, laying the foundation for the development of alternatives to conventional antibiotics.

Methods

Ethics statement

All the animal experiments were approved by the Animal Ethics Committee of Zhengzhou University in accordance with the guidelines of the Animal Welfare and Research Ethics Committee.

Peptides synthesis

MPX (H-INWKGIAAMAKKLL-NH2) was synthesized and purified by Ji er sheng hua (Shanghai, China). The purity of MPX was higher than 98%, as determined by high-performance liquid chromatography (HPLC) and mass spectrometry. MPX was dissolved in ddH_2O and stored at -20 °C.

Preparation of E.coli strain

E. coli was obtained from the China Institute of Veterinary Drug Control (Beijing, China). The *E. coli* strain was seeded on LB (Solarbio, China) agar to obtain single pure colonies. Then, a single colony of *E. coli* was inoculated into LB broth and incubated overnight at 37 °C and 180 rpm/min. 100 μL were transferred to 10 mL fresh LB broth and incubated at 37 °C and 180 rpm/min for 4 h. Then, 1 mL cultures were collected and washed twice with phosphate buffer (pH = 7.4) at 8000 rpm/min for 5 min. Then, ten times serial dilutions were performed and seeded on LB agar to obtain single pure colonies, and 4.5×10^7 CFU/mL bacteria were used.

Cell culture

IPEC-J2 cells were cultured in DMEM with 10% fetal bovine serum and 1% antibiotics (penicillin and streptomycin) and incubated in an environment at 37 °C with 5% CO_2. At 90% confluence, the cells were digested by trypsin and cultured in six-well cell plates (Solarbio, China). When they reached 80–90% confluence, the cells were cultured in DMEM medium without 1% antibiotics and then treated with MPX (10 μg/mL) for 2 h. Then, the cells were further cultured with *E. coli* (MOI = 10) for 12 h.

Cytotoxicity studies

Cell viability was determined by the CCK-8 kit (Meilunbio, China). The experiments were carried out in accordance with the instructions. First, IPEC-J2 cells were cultured in 96-well plates at 1×10^4 cells/well and treated with the indicated concentration (2-512 μg/mL) of MPX for 24 h. Then, the IPEC-J2 cells were incubated with 10 μL CCK-8 per well in a cell culture incubator for 2 h. Then, a microplate reader was used to detect the absorbance of each well at 450 nm (Dynatech Laboratories, USA). Three replicates per sample were assessed.

The LDH release assay (Nanjing Jiancheng, China) was used to determine whether MPX caused IPEC-J2 cell membrane damage. The experiments were carried out in accordance with the instructions. Briefly, IPEC-J2 cells were cultured in 96-well plates at 1×10^4 cells/well and treated with the indicated concentration (2-512 μg/mL) of MPX in an environment at 37 °C with 5% CO_2 for 24 h. In addition, IPEC-J2 cells were pretreated with MPX (10 μg/mL) for 2 h and infected with *E. coli* (MOI = 10) for different times (3 h, 6 h, 12 h, 24 h). The optical densities were measured at 450 nm using a microplate reader (VARIOSKAN FLASH, USA). Three replicates per sample were assessed.

Real- time PCR

The primer sequences for real- time PCR are shown in Table 1. Total RNA was extracted using RNA extraction kit reagent (Soliabao, China). The quantity and quality of the RNA were determined using a NanoDrop 2000 spectrophotometer (Thermo Fisher Scientific, USA). cDNA was obtained using a reverse transcription kit (Thermo Scientific Molecular Biology, USA). Each reaction (10 μL) volume included 5 μL SYBR Green Master Mix (QuantiNova, China), 0.5 μL forward primer (10 μM), 0.5 μL reverse primer (10 μM), 0.5 μL cDNA and 3.5 μL ddH_2O. The thermocycler reaction included 2 min at 95 °C and 40 cycles

of 20 s at 95 °C and 30 s at 60 °C, and melt curves were added. The housekeeping gene was GAPDH. The $2^{-\Delta\Delta Ct}$ method was used to calculate the relative mRNA expression [11]. Three replicates per sample were assessed.

Table 1
The primer sequences for real-time PCR

Genes	Sequence
MUC2	F:5'- CTGCTCCGGGTCCTGTGGGA-3'
	R:5'- CCCGCTGGCTGGTGCGATAC-3'
TNF-α	F:5' -CTCATGCACCACCATCAAGG-3'
	R:5'-ACCTGACCACTCTCCCTTTG-3'
IL-6	F:5' -CTCTGGCGGAGCTATTGAGA-3'
	R:5'-AAGTCTCCTGCGTGGAGAAA-3'
IL-2	F:5'-CCTGAGCAGGATGGAGAATTACA-3'
	R:5'-TCCAGAACATGCCGCAGAG-3'
Occludin	F:5' -ACGGACCCTGACCACTATGA-3'
	R:5'- TCAGCAGCAGCCATGTACTC-3'
Claudin-1	F:5' - AGCTGCCTGTTCCATGTACT-3'
	R:5'- CTCCCATTTGTCTGCTGCTC-3'
ZO-1	F:5'-ACCCGAAACTGATGCTGTGGATAG-3'
	R:5'-AAATGGCCGGGCAGAACTTGTGTA-3'
GAPDH	F:5'-TGGAGAAACCTGCCAAGTATGA-3'
	R:5'-TGGAAGAATGGGAGTTGCTGT-3'

Western blotting

Total protein was extracted with RIPA lysate buffer (KeyGEN, China). The protein concentration was determined using a BCA protein content kit (Biyuntian, China). Then, the proteins in the lysate supernatants were separated by 10% SDS-PAGE and transferred onto a PVDF membrane. After blocking with 5% bovine serum albumin (BSA) for 2 h, the membrane was incubated with primary antibodies overnight at 4 °C and washed with TBST 5 times for 7 min each time. The membranes were incubated with horseradish peroxidase (HRP)-conjugated secondary antibodies for 1 h at room temperature. The membranes were washed with TBST 5 times for 7 min each time [12]. The bands were detected using ECL (Solaibao, China). ImageJ software was used to quantify the band intensities. Primary antibodies against β-actin (Abcam, USA) and occludin (Abcam, USA) were used in this study.

Transmission Electron Microscopy

The tight junctions (TJs) and microvillus morphology between the intestinal epithelial cells of mice were observed by TEM [13]. Mouse jejunum specimens were obtained with a scalpel and fixed in 2.5% glutaraldehyde for 12 h at 4 °C. Then, the jejunum of the mice was treated with osmic acid and embedded in epon. Ultrathin sections were acquired using a diamond knife and then stained with uranyl acetate and lead citrate before being observed by TEM (7610plus/FEI Apreo, Japan).

Scanning Electron Microscopy

The morphology of the jejunum villi and microvilli in mice was observed by SEM [14]. Jejunum tissue from the mice was fixed with 2.5% glutaraldehyde overnight at 4 °C and then incubated with 1% OsO_4 for 1 h. The jejunum specimens from the mice were then dehydrated with an ethanol gradient (30%, 50%, 70%, 80%, 90%, 95% and 100%) for 15 min at each step and then treated with a mixture of alcohol and isoamyl acetate (v:v = 1:1) for 30 min. Then, isoamyl acetate was added for 1 h. Then, the dehydrated specimens were coated with gold-palladium and visualized using a Philips Model SU8010 FASEM (HITACHI, Japan).

ELISA

The serum levels of interleukin-6 (IL-6), tumor necrosis factor-alpha (TNF-α) and interleukin-2 (IL-2) were determined using ELISA kits (Biolegend, USA). In addition, the serum level of myeloperoxidase (MPO) was detected using an ELISA kit (Multi Science, China). All the samples were measured according to the manufacturers' instructions. Three replicates per sample were assessed.

Histopathology and immunohistochemistry

The jejunum and colon tissues of the mice were fixed in 4% paraformaldehyde for 24 h and embedded in paraffin. Hematoxylin and eosin (H&E) staining was used to stain the jejunum. Images were obtained using a DM3000 microscope (PHASE CONTRAST, Japan). Image-Pro software (Media Cybernetics, USA) was used to measure the villous height and crypt depth, and then, the ratio of villous height to crypt depth was calculated [15].

For immunohistochemistry (IHC), 5-μm sections of the jejunum and colon tissues were embedded in paraffin. The sections were incubated in sodium citrate buffer (pH = 6.0) to repair the antigens and placed in 3% hydrogen peroxide solution to block endogenous peroxidase after dewaxing and rehydration. To block nonspecific binding sites, the sections were incubated with 3% BSA for 30 min. Then, the sections were incubated with anti-p-p38, anti-p-pERK, and anti-p-pJNK antibodies overnight at 4 °C. Then, HRP-conjugated secondary antibodies were added to the sections and incubated for 50 min. Next, the sections were counterstained with hematoxylin after development with DAB buffer [16].

Immunofluorescence

IPEC-J2 cells were cultured in special plates for confocal laser microscopy, pretreated with MPX (10 μg/mL) for 2 h and then incubated with *E. coli* (MOI = 10) at 37 °C for 12 h. Then, the IPEC-J2 cells were washed with PBS (pH = 7.4) 3 times and then fixed with 2.5% glutaraldehyde for 30 min. The IPEC-J2 cells were washed 3 times in PBS (pH = 7.4), blocked with 5% bovine serum albumin at room temperature for 1 h, incubated with primary rabbit antibodies overnight at 4 °C (anti-occludin, anti-p-p38, and anti-p-p65), incubated with the secondary antibody (Alexa Fluor 594-anti-rabbit) for 1 h and stained with DAPI for 15 min. Tight junction proteins and inflammatory proteins were observed under a confocal laser microscopy (EVOS M7000, USA) [17].

Animals and sample collection

A total of 50 BALB/c mice (6 to 8 weeks old, body weights of 18 to 20 g, female) were purchased from Zhengzhou University. The animals were random divided into 4 experimental groups, including the control, *E. coli*, *E. coli* + MPX, and *E. coli* + Enro groups, with 10 mice per group. The each BALB/c mice were challenged with intraperitoneal injection of *E. coli*(4.5×10^7 CFU/mL) [18]. The mice were treated with intraperitoneal injection of normal saline (control), MPX (20 mg/kg), or Enro (20 mg/kg) once a day for 3 d after infection with *E. coli* for 2 h. The clinical symptoms of the mice, including the state of the hair, body weight change, mental state, and appetite, were recorded every day. The specific scoring criteria were as follows: no clinical signs as 0; slight as 1; moderate as 2; severe as 3. The mice were sacrificed at 96 h after *E. coli* infection. The serum was used for inflammatory factor analysis. The liver, spleen, lung and intestines were collected and fixed with 4% paraformaldehyde for H&E staining, immunohistochemistry and immunofluorescence analysis. Glutaraldehyde (2.5%) was used to fix the jejunum to observe the changes in the intestinal villi and microvilli by scanning electron microscopy and transmission electron microscopy.

Statistical analysis

Statistical analysis was implemented using GraphPad Prism software (version 8.0, La Jolla, CA, USA). All the results are expressed as the mean ± S.E.M. Group comparisons were performed by one-way analysis of variance (ANOVA) followed by Tukey's test. Statistical significance was expressed using $P < 0.05$. *$P < 0.05$;**$P < 0.01$; ***$P < 0.001$; $^{\#}P < 0.05$, $^{\#\#}P < 0.01$, $^{\#\#\#}P < 0.001$.

Results

MPX reduces the release of LDH and inhibits the expression of inflammatory cytokines

The cytotoxicity of MPX was tested since the aim of this study was to develop this peptide as a safe alternative to antibiotics. A CCK-8 kit was used to determine the viability of IPEC-J2 cells after treatment with MPX at different concentrations (2-512 μg/mL) for 24 h. Compared with the control treatment, MPX increased the cell viability (Fig. 1a, $P < 0.001$). The effect on cultured cells was not significant, even at a high concentration of 128 μg/mL. Interestingly, the results showed that low concentrations of MPX could promote the growth of IPEC-J2 cells ($P < 0.05$). The release of LDH was examined to further determine the toxicity of MPX. Compared with the control group, treatment with different concentrations (2-512 μg/mL)

of MPX for 24 h did not significantly increase the release of LDH, even at a concentration of 128 μg/mL (Fig. 1b). Moreover, the LDH release from IPEC-J2 cells was notably reduced after pretreatment with MPX for 2 h prior to infection with *E. coli* (Fig. 1c, $p < 0.05$). These results indicated that MPX maintained the cellular membrane integrity of IPEC-J2 cells.

The increased expression of inflammatory factors, such as IL-2, IL-6 and TNF-α, is closely related to the inflammatory response [19]. To evaluate the anti-inflammatory effects of MPX after *E. coli* infection, the expression of IL-2, IL-6 and TNF-α was determined by real- time PCR. Compared with *E. coli* alone, treatment with MPX significantly inhibited the *E. coli*-induced mRNA expression of IL-2, IL-6 and TNF-α (Fig. 1d, e and f, $p < 0.05$). In addition, the confocal laser microscopy results showed that *E. coli* infection significantly increased the expression of p-p38, p-p65 and TLR4, while pretreatment with MPX significantly decreased the expression of p-p38, p-p65 and TLR4 (Fig. 1g), indicating that MPX could inhibit the release of inflammatory cytokines by reducing the phosphorylation of p38 and the activation of p65 and TLR4.

Figure 1 MPX does not induce cytotoxicity and alleviates inflammation in IPEC-J2 cells. (**a**) Cell viability was measured using the CCK-8 assay, IPEC-J2 cells were cultured with different concentrations (2-512 μg/mL) of MPX for 24 h; (**b**) The release of LDH from IPEC-J2 cells after treatment with different concentrations (2-512 μg/mL) of MPX for 24 h; (c) MPX decreased the *E. coli*-induced release of LDH from IPEC-J2 cells (MOI = 10) at different times; (**d-f**) The mRNA expression of IL-2, IL-6 and TNF-α after MPX treatment. (**g**) The expression of p-p38, p-p65 and TLR4 in IPEC-J2 cells assessed by confocal laser microscopy. $^{\#}P < 0.05$; $^{\#\#}P < 0.01$; $^{\#\#\#}P < 0.001$ *E. coli* vs control; $^{*}P < 0.05$;$^{**}P < 0.01$; $^{***}P < 0.001$ MPX treatment vs *E. coli*.

MPX inhibits E. coli**-induced tight junction damage in IPEC-J2 cells**

Tight junctions are the structure connecting adjacent epithelial cells, and these junctions have a sealing effect on the intercellular space and prevent toxic and harmful substances in the intestinal cavity from entering the submucosa through the epithelial cell gap. Tight junctions are composed of a variety of tight junction proteins, including ZOs, occludin, and claudins [20]. To evaluate the effects of MPX after *E. coli* infection, the expression of ZO-1, occludin, and claudin-1 was determined by real-time PCR. As shown in Fig. 2A, the *E. coli*-induced mRNA expression of ZO-1 and occludin in IPEC-J2 cells was significantly increased after MPX treatment ($p < 0.05$), while the expression of claudin-1 was not significantly altered ($p > 0.05$). Interestingly, in a wound healing assay, the wound width was significantly reduced at 48 h in IPEC-J2 cells treated with MPX (Fig. 2b, $p < 0.01$), indicating that MPX is beneficial for healing the damage caused to intestinal epithelial cells. Furthermore, western blot and immunofluorescence analyses were used to investigate the effects of MPX on the tight junction proteins in IPEC-J2 cells after *E. coli* infection. As shown in Fig. 2c, d, compared with the control treatment, MPX significantly increased the expression of occludin in IPEC-J2 cells. Moreover, the expression of occludin induced by *E. coli* was significantly increased after treatment with MPX. The results suggested that MPX could significantly increase the tight junction protein expression induced by *E. coli* in IPEC-J2 cells.

Figure 2 MPX enhances IPEC-J2 cell barrier function. (**a**) The *E. coli*-induced mRNA expression of ZO-1, occludin and claudin-1 in IPEC-J2 cells after treatment with MPX; (**b**) IPEC-J2 cells were incubated with medium alone or MPX (10 μg/mL) in a wound healing assay. Images were obtained at 0 h, 48 h and 96 h, and the wound width was measured at 48 h; (**c**) The *E. coli*-induced protein level of occludin in IPEC-J2 cells after pretreatment with MPX was determined by western blotting; (**d**) The effect of MPX on the expression of occludin in IPEC-J2 cells was assessed by confocal laser microscopy. $^{\#}P < 0.05$; $^{\#\#}P < 0.01$; $^{\#\#\#}P < 0.001$ *E. coli* vs control; *P < 0.05;**P < 0.01; ***P < 0.001 MPX treatment vs *E.coli*.

MPX protects mice against fatal infection with E. coli

The therapeutic effect of MPX on intestinal inflammation and the intestinal barrier was evaluated in a BALB/c mouse model. The results showed that MPX could protect the mice against infection with a lethal dose of *E. coli*, and the survival rate of the mice was 90%; this effect of MPX was better than that of Enro. However, the mice infected with *E. coli* without MPX treatment all died within 60 h (Fig. 3a). The observation of clinical symptoms revealed that *E. coli* infection caused severe diarrhea, lack of energy, loss of appetite, clustering, and messy back hair, while these symptoms were significantly alleviated after MPX treatment; these effects of MPX were superior to the effects of the same dose of Enro (Fig. 3b). The weight of the mice infected with *E. coli* was notably reduced (Fig. 3c, $p < 0.01$), but it was significantly increased after MPX and Enro treatment (Fig. 3c, $p < 0.01$) and not significantly different from the control (Fig. 3c, $p > 0.05$). The weights of the livers and spleens in the *E. coli* infection group were notably heavy (Fig. 3d, e, $p < 0.05$) and significantly decreased after MPX treatment; after MPX treatment, these weights were not significantly different from those in the control group (Fig. 3d, e, $P > 0.05$). The weight of the lung was not significantly changed after *E. coli* infection (Fig. 3f, $P > 0.05$). The colonization of *E. coli* in the liver, spleen, lung and feces of the mice was examined by counting on LB agar plates. The results showed that the number of bacteria colonizing the spleens of the *E. coli* group was greater than that colonizing the liver and lung, and this number was significantly decreased after MPX and Enro treatment (Fig. 3g, $P < 0.05$). The number of bacteria colonizing the feces was significantly lower after MPX and Enro treatment than after infection with *E. coli* alone (Fig. 3h, $P > 0.05$). These results indicated that MPX exerted good antibacterial effects in vivo and protected against lethal infection with *E. coli* in mice.

Figure 3 MPX protects mice against infection with a lethal dose of *E. coli*. (**a**) The survival rate of mice infected with *E. coli* after MPX treatment; (**b**) The clinical symptom score of mice infected with *E. coli* after MPX treatment; (**c**) The weight of mice infected with *E. coli* after MPX treatment; (**d**-**f**) The weight of the liver, spleen and lung of mice infected with *E. coli* after MPX treatment; (**g**) The number of bacteria in the liver, spleen and lung of mice infected with *E. coli* after MPX treatment; (**h**) The number of bacteria in the feces of mice infected with *E. coli* after MPX treatment. Control group, mice injected with sterile saline; *E. coli* group, mice injected with *E. coli*; MPX group, mice treated with intraperitoneal injection MPX and injected with *E. coli*. $^{\#}P < 0.05$; $^{\#\#}P < 0.01$; $^{\#\#\#}P < 0.001$ *E. coli* vs control; *P < 0.05;**P < 0.01; ***P < 0.001 MPX and Enro treatment vs *E. coli*.

MPX reduces the levels of inflammatory cytokines and improves intestinal morphology

MPO activity is an index of neutrophil infiltration and inflammation, and MPO can produce specific oxidative species [21]. To evaluate the effect of the MPX-mediated anti-inflammatory response after *E. coli* infection, the levels of IL-2, IL-6, TNF-α and MPO were detected by ELISA. As shown in Fig. 4a, the levels of the inflammatory factors IL-2, IL-6, TNF-α and MPO were significantly increased after *E. coli* infection, while MPX significantly reduced the secretion of IL-6 ($p < 0.01$), IL-2, TNF-α and MPO ($p < 0.05$). H&E staining was used to explore the effect of MPX on the intestinal morphology of the jejunum in mice infected with *E. coli*; the results showed that infection with *E. coli* caused typical intestinal inflammation and barrier damage, shortened villi, necrosis, large amounts of inflammatory cell infiltration into the jejunum and disrupted intestinal villi, while MPX treatment increased villous height and goblet cell counts and decreased the infiltration of leukocytes into the jejunum, and these levels were not significantly different compared with those observed in control group (Fig. 4b). Moreover, compared with *E. coli* infection alone, MPX treatment increased the villi length in the jejunum in the mice, decreased the crypt depth, and increased the ratio of villi height to crypt depth, and these effects of MPX were better than those of Enro (Fig. 4c, $p < 0.05$). These results suggest that MPX effectively reduced inflammatory factor secretion and improved intestinal morphology and integrity in mice infected with *E. coli*.

Figure 4 MPX inhibits inflammatory cytokine expression and improves intestinal morphology. (**a**) The levels of inflammatory cytokines (IL-2, IL-6 and TNF-α) and MPO in mouse serum were detected using ELISA; (**b**) The jejunum of mice was stained with H&E (bars, 100 μm); images were obtained at 200 × magnification; (**c**) The length of jejunal villi, the depth of crypts, and the ratios of villi length to crypt depth were detected by ipwin32 software. $^{\#}P < 0.05$; $^{\#\#}P < 0.01$; $^{\#\#\#}P < 0.001$ *E. coli* vs control; $^{*}P < 0.05$; $^{**}P < 0.01$; $^{***}P < 0.001$ MPX and Enro treatment vs *E. coli*.

MPX improves intestinal villi and microvilli

Previous H&E staining studies have shown that *E. coli* infection could damage the intestinal morphology of the jejunum in mice. SEM and TEM were used to further evaluate the effects of MPX on the intestinal morphological changes induced by *E. coli*. The SEM results showed that *E. coli* infection caused severe damage to the morphology of the intestinal villi and destruction of the integrity of the intestinal villi, while MPX treatment obviously alleviated the injury to the jejunum villi and microvilli, as observed at high (200×) and low (30.000×) magnifications (Fig. 5a); this effect of MPX was better than that of Enro, which was consistent with H&E staining. We further evaluated the effect of MPX on the microvilli and tight junction proteins of intestinal epithelial cells by TEM. The results showed that *E. coli* infection caused microvilli to fall off, decreased the number of microvilli, and damaged the tight junction structure of the intestinal epithelial cells, while MPX treatment significantly increased the quantity of the microvilli in intestinal epithelial cells; this effect of MPX was better than that of Enro, and the results were not significantly different compared with those observed in the control group (Fig. 5b). These results indicate that MPX could protect against *E. coli*-induced damage to jejunal villi and microvilli in intestinal epithelial cells.

Figure 5 MPX improves the intestinal morphology of the jejunum and the microvilli of intestinal epithelial cells. (**a**) Morphological changes in the jejunum villi were observed by SEM (upper, 200×; lower, 30,000×);

(**b**) Morphological changes in the microvilli and tight junction proteins in intestinal epithelial cells were observed by TEM (upper, 1500×; lower, 3000×).

MPX suppresses intestinal inflammation by downregulating the expression of p-p38 and p-p65

Previous studies showed that MPX treatment could reduce the serum levels of inflammatory factors after *E. coli* infection. To further investigate the anti-inflammatory effect of MPX on the intestine, the mRNA expression of IL-2, IL-6 and TNF-α in the jejunum and colon was detected using real-time PCR. *E. coli* infection led to a significant increase in the expression of the inflammatory factors IL-2, IL-6 and TNF-α in the jejunum and colon (Fig. 6a, $p < 0.01$), while MPX and Enro treatment significantly inhibited the mRNA expression of IL-2, IL-6 and TNF-α in the jejunum ($p < 0.01$) and colon ($p < 0.05$); after MPX and Enro treatment, the levels were not significantly different from those observed in the control group ($P > 0.05$). Mitogen-activated protein kinases (MAPKs), including JNK, ERK1/2 and p38, are a group of serine/threonine proteins and the final step of cytoplasmic signal transduction pathways that are activated by multiple extracellular signal pathways. These proteins play a role in the activation of nuclear transcription factor p65, regulating gene expression and participating in cytokine secretion and apoptosis after activation [22]. Immunohistochemistry and immunofluorescence were used to further explore the mechanism by which MPX inhibits the secretion of inflammatory factors. The immunohistochemistry results showed that MPX notably reduced the expression of p-p38 in the crypts of the jejunum, and this effect was superior to the effects of the same dose of Enro (Fig. 6b). However, the expression of p-pJNK and p-pERK in the jejunum was not significantly changed after treatment with MPX and Enro (Fig. 6b), indicating that MPX had no significant effect on the expression of p-pJNK and p-pERK and mainly regulated the p-p38 signaling pathway, decreasing the secretion of inflammatory factors and thereby reducing the inflammatory response. The results were consistent with Fig. 1g. In addition, the activation of p65 was analyzed by immunofluorescence, and the results showed that MPX significantly decreased the phosphorylation of p65 compared with *E. coli* infection alone (Fig. 6c). These results indicated that MPX could inhibit the release of inflammatory cytokines by reducing the phosphorylation of p38 and the activation of p65.

Figure 6 MPX suppresses intestinal inflammation by inhibiting the activation of the MAPK and P65 signaling pathways. (**a**) The mRNA expression of IL-2, IL-6, and TNF-α in the jejunum and colon after MPX treatment was measured by real-time PCR; (**b**) The expression of p-p38, p-pJNK and p-pERK in the jejunum after MPX treatment was determined by immunohistochemistry (bars, 100 μm); (**c**) The effect of MPX on the expression of p-p65 in the colon was assessed by immunofluorescence. $^{\#}P < 0.05$; $^{\#\#}P < 0.01$; $^{\#\#\#}P < 0.001$ *E. coli* vs control; $^{*}P < 0.05$; $^{**}P < 0.01$; $^{***}P < 0.001$ MPX and Enro treatment vs *E.coli*.

MPX enhances the expression of intestinal tight junction proteins and mucin

Mucin is the key matrix-forming component of mucus, which is an innate protective barrier that protects the host from pathogenic attack [23]. The IPEC-J2 cells results showed that MPX could improve tight junction protein expression after *E. coli* infection. Immunofluorescence and real-time PCR were used to further investigate the effects of MPX on *E. coli*-induced tight junction protein and MUC2 expression in the jejunum and colon. The results showed that *E. coli* infection decreased the expression of ZO-1, occludin and MUC2, while MPX treatment significantly increased the expression of ZO-1, occludin and

MUC2 in the jejunum and colon; this effect of MPX was superior to that of Enro (Fig. 7a, $P < 0.05$). However, none of the groups showed a significant effect on the expression of the tight junction protein claudin-1 (Fig. 7a, $P > 0.05$). Immunofluorescence was used to further study the effect of MPX on tight junction protein and MUC2 expression after *E. coli* infection. The results showed that *E. coli* infection reduced the expression of ZO-1, occludin and MUC2 in the jejunum and colon of mice, while the expression of ZO-1, occludin and MUC2 was improved after treatment with MPX. The effect was better than that of Enro, and the expression levels were not significantly different from those observed in the control group (Fig. 7b, c). Collectively, these results indicate that MPX treatment could significantly improve the expression of tight junction proteins and mucin in the jejunum and colon.

Figure 7 MPX improves the expression of tight junction proteins and mucin in the jejunum and colon. (**a**) The mRNA expression of claudin-1, ZO-1, occludin and MUC2 in the jejunum and colon; (**b**) The protein expression of claudin-1, occludin, ZO-1 and MUC2 (red) and DAPI (blue) in the jejunum; (**c**) The protein expression of claudin-1, occludin, ZO-1 and MUC2 (red) and DAPI (blue). Scale bar = 10 μm.

Figure 8 MPX regulates epithelial cells and in vivo signaling pathways.

Discussion

Antimicrobial peptides are considered to be the best substitutes for antibiotics due to their beneficial antibacterial, anti-inflammatory, and immune regulatory effects and have become a focus of research in recent years [24]. MPX belongs to the mastoparan family, contains 14 amino acids, has a high concentration in wasp venom, and has good antimicrobial activity against bacteria, indicating that MPX can be used as a substitute for antibiotics in the treatment of bacterial infection [9]. In this study, we found that MPX exhibited almost no cytotoxicity in IPEC-J2 cells, significantly reduced the expression of IL-2, IL-6 and TNF-α induced by *E. coli*, increased the expression of ZO-1 and occludin in intestinal epithelial cells, and promoted the wound healing of intestinal epithelial cells. The therapeutic effect of MPX was evaluated in a murine model, and the results showed that MPX could protect against lethal infection with *E. coli* in mice and reduce the expression of the inflammatory factors IL-2, IL-6 and TNF-α, thereby alleviating intestinal inflammation. In addition, MPX improved intestinal morphology and enhanced intestinal barrier function. This study was the first to evaluate the effect of MPX against *E. coli* infection in vitro and in vivo, laying a foundation for the treatment of intestinal diseases with MPX.

Previous studies have found that the morphological integrity of villi and microvilli, which plays a key role in the absorption of intestinal nutrients, is an important indicator of the performance and health of the host [25]. Yoon et al investigated the effect of the addition of the antimicrobial peptide cLFchimera (20 mg/kg) to the diet of broiler chickens in the context of necrotic enteritis (NE) challenge and found that cLFchimera ameliorated intestinal lesions and changes to villus morphology in the jejunum [26]. Liang et al found that bovine antimicrobial peptide-13 (APB-13) has good antiviral activity against transmissible gastroenteritis virus (TGEV) and significantly reduced the piglet diarrhea induced by TGEV, improving intestinal villus morphology [27]. Previous studies have found that the antimicrobial peptide MccJ25

could protect against ETEC infection and significantly alleviate the destruction of intestinal morphology and changes in villus morphology in mice infected with ETEC [3]. Wang et al investigated the effect of the antimicrobial peptide JH-3 on the intestinal inflammation induced by *Salmonella* CVCC541 and found that JH-3 could effectively alleviate the pathological damage to the duodenum and jejunum, reduce the loss of intestinal villi and improve the morphology of intestinal villi [28]. In this study, the results showed that MPX could significantly improve the pathological damage to the intestinal caused by *E. coli*, reduce the loss of intestinal villi, and maintain the morphology of intestinal villi. The effects of MPX on the intestinal epithelial cell microvilli were further confirmed using TEM, and MPX not only improved the morphology of intestinal villi but also increased the number of microvilli, thereby increasing nutrient absorption in the intestine. These results indicated that MPX could effectively alleviate intestinal damage and maintain villi and microvilli morphology, promoting nutrient absorption in the intestine.

Antimicrobial peptides, as an important part of the natural immune system, possess good anti-inflammatory activity [29]. Long-term and excessive production of proinflammatory cytokines may lead to intestinal damage and high energy requirements [30]. Atikan Wubulikasimu et al found that the antimicrobial peptide AKK8 possessed good antibacterial activity against drug-resistant strains of *C. albicans*, significantly reducing the levels of IL-6, IL-1β and TNF-α in the serum of mice infected with *C. albicans* [31]. Ding et al evaluated the effect of the antimicrobial peptide microcin J25 against ETEC infections in a murine model and found that microcin J25 decreased the secretion of inflammatory factors by inhibiting the activation of the MAPK and NF-κB signaling pathways, thereby alleviating the intestinal inflammatory response induced by ETEC [3]. Min Kyoung Shin et al investigated the effect of the antimicrobial peptide Lycotoxin-Pa4a on the LPS-induced inflammatory response in RAW264.7 cells and found that Lycotoxin-Pa4a significantly reduced the expression of the inflammatory cytokines IL-1β and TNF-α by inhibiting the activation of the MAPK pathway, thereby inhibiting the LPS-induced inflammatory response in RAW264.7 cells [32]. In this study, we found that MPX significantly reduced *E. coli*-mediated expression of the inflammatory factors IL-2, IL-6 and TNF-α by inhibiting the activation of p-p38 and p-p65 in vitro and in vivo, thereby attenuating intestinal inflammation. These results indicated that MPX exerts good anti-inflammatory effects and can be a beneficial agent for alternative antibiotics.

The intestinal barrier mainly includes the intestinal epithelial barrier, immune barrier, chemical barrier and biological barrier. In addition, the intestinal epithelial barrier is the first barrier that can prevent bacteria, antigens and other toxic and harmful substances from entering the submucosa of the intestine and blood [33]. The tight junction (TJ) structure is composed of TJ proteins, such as ZO-1, occludin and claudins, which are an important part of the intestinal epithelial barrier and play an important role in intestinal epithelial cells [34]. Lin et al investigated the effect of the antimicrobial peptide gloverin A2 (BMGlvA2) on ETEC-induced intestinal barrier disruption in mice and found that BMGlvA2 clearly improved the expression of the tight junction protein ZO-1 in the intestine after ETEC infection [35]. Zhang et al found that the hybrid peptide LL-37-Tα1 (LTA) could increase the LPS-induced expression of ZO-1 and occludin in the jejunum of mice, improving intestinal barrier function [36]. Yu et al explored the therapeutic effects of the recombinant antimicrobial peptide microcin J25 on epithelial barrier dysfunction in a murine model and found that MccJ25 could enhance the expression of tight junction proteins, attenuating ETEC-

induced intestinal barrier dysfunction [37]. In this study, we found that MPX improved the expression of ZO-1 and occludin in IPEC-J2 cells. Furthermore, MPX enhanced the expression of the tight junction proteins ZO-1, occludin and MUC2 in the jejunum and colon in mice, indicating that MPX attenuates intestinal barrier dysfunction by improving tight junction protein and mucin expression. Surprisingly, MPX is more effective in increasing tight junction protein and mucin expression than Enro. The reason may be due to the antibacterial properties of antibiotics, which control the balance of microorganisms in the intestine.

Conclusion

In summary, as shown in Fig. 8, we demonstrated that MPX could reduce *E. coli* growth, attenuate the inflammatory response and intestinal damage, inhibit *E. coli*-induced TLR4 expression, and decrease the IL-2, IL-6 and TNF-α levels by blocking the activation of the p65 and p38 inflammatory pathways in vitro and in vivo. In addition, MPX improved intestinal barrier function and increased the expression of the tight junction proteins ZO-1, occludin and mucin. These findings suggest that MPX can be an excellent antimicrobial or anti-inflammatory agent to protect against pathogen infections, laying a foundation to develop MPX as a substitute for conventionally used antibiotics or drugs.

Abbreviations

MPX
Antimicrobial peptide MPX; *E. coli*:*Escherichia coli* O157:H7; Enro:Enrofloxacin; IL-2:Interleukin-2; IL-6:Interleukin-6; TNF-α:Tumor necrosis factor; LDH:Lactate dehydrogenase; MPO:Myeloperoxidase; MUC2:Mucin 2; SEM:Scanning Electron Microscopy; TEM:Transmission Electron Microscopy; H&E:Hematoxylin and eosin.

Declarations

Acknowledgments

The authors thank Qing Wang for providing the instrument. Bolin Hang and Yawei Sun for their help and guidance with the lab work.

Authors' contributions

XQZ and LW contributed equally to this work. XQZ performed laboratory experiments, and statistical analysis and drafted the manuscript. LW, HF and JHH assisted in study design and reviewed manuscript; CLZ, XJX, SPZ, and YMW assisted in laboratory work, collection and analysis of data; HHZ, YZX, SJC, and JQJ contributed to study design and reviewed the manuscript; and YYB, YHH, GPZ statistical analyses and critically reviewed the manuscript. The authors read and approved the final manuscript.

Funding

This work was supported by the National Natural Science Foundation of China (No. 31702259 and 31520103917), Young Talent Lifting Project in Henan Province (2020HYTP041), Key Scientific Research Projects of Colleges and University in Henan Province (21A230004), Climbing Project of Henan Institute of Science and Technology (2018JY02) and Program for Innovative Research Teams (in Science and Technology) at the University of Henan Province (20IRTSTHN025).

Availability of data and materials
Data may be provided following request to the corresponding author.

Consent for publication
Not applicable.

Competing interests
All authors declare that there are no conflicts of interest.

Author details

[1] College of Animal Science and Veterinary Medicine, Henan Institute of Science and Technology, Xinxiang 453003, China

[2] Faculty of Veterinary Medicine, Sumy National Agrarian University, Sumy, Ukraine

[3] College of Animal Science and Veterinary Medicine, Henan Agricultural University,

Zhengzhou 450000, China

References

1. Glombowsky P, Campigotto G, Galli GM, Griss LG, Da RG, Lopes MT, et al. Experimental infection with Escherichia coli in broilers: Impacts of the disease and benefits of preventive consumption of a stimulator of homeopathic immunity. Microb Pathog. 2020;149:104570.
2. Chen S, Wu X, Xia Y, Wang M, Liao S, Li F, et al. Effects of dietary gamma-aminobutyric acid supplementation on amino acid profile, intestinal immunity, and microbiota in ETEC-challenged piglets. Food Funct. 2020;11(10):9067-74.
3. Ding X, Yu H, Qiao S. Lasso peptide microcin j25 effectively enhances gut barrier function and modulates inflammatory response in an enterotoxigenic escherichia coli-Challenged mouse model. Int J Mol Sci. 2020;21(18):6500.
4. Smith MG, Jordan D, Gibson JS, Cobbold RN, Chapman TA, Abraham S, et al. Phenotypic and genotypic profiling of antimicrobial resistance in entericEscherichia colicommunities isolated from finisher pigs in Australia. Aust Vet J. 2016;94(10):371-6.
5. Alfei S, Schito AM. From nanobiotechnology, positively charged biomimetic dendrimers as novel antibacterial agents: A review. Nanomaterials-Basel. 2020;10(10):2022.

6. Faya M, Hazzah HA, Omolo CA, Agrawal N, Maji R, Walvekar P, et al. Novel formulation of antimicrobial peptides enhances antimicrobial activity against methicillin-resistant Staphylococcus aureus (MRSA). Amino Acids. 2020;52(10):1439-57.
7. Lee H, Lee J, Park Y, Kim JH, Eickelberg O, Yang S. WKYMVm ameliorates acute lung injury via neutrophil antimicrobial peptide derived STAT1/IRF1 pathway. Biochem Bioph Res Co. 2020;533(3):313-8.
8. Leite NB, Leite NB, Da Costa LC, Da Costa LC, Dos Santos Alvares D, Dos Santos Alvares D, et al. The effect of acidic residues and amphipathicity on the lytic activities of mastoparan peptides studied by fluorescence and CD spectroscopy. Amino Acids. 2011;40(1):91-100.
9. Henriksen JR, Etzerodt T, Gjetting T, Andresen TL. Side chain hydrophobicity modulates therapeutic activity and membrane selectivity of antimicrobial peptide mastoparan-X. Plos One. 2014;9(3):e91007.
10. Wang L, Zhao X, Zhu C, Zhao Y, Liu S, Xia X, et al. The antimicrobial peptide MPX kills Actinobacillus pleuropneumoniae and reduces its pathogenicity in mice. Vet Microbiol. 2020;243:108634.
11. Omonijo FA, Liu S, Hui Q, Zhang H, Lahaye L, Bodin J, et al. Thymol improves barrier function and attenuates inflammatory responses in porcine intestinal epithelial cells during lipopolysaccharide (LPS)-Induced inflammation. J Agr Food Chem. 2018;67(2):615-24.
12. Xin C, Kim J, Quan H, Yin M, Jeong S, Choi J, et al. Ginsenoside Rg3 promotes Fc gamma receptor-mediated phagocytosis of bacteria by macrophages via an extracellular signal-regulated kinase 1/2 and p38 mitogen-activated protein kinase-dependent mechanism. Int Immunopharmacol. 2019;77:105945.
13. Narayana JL, Huang H, Wu C, Chen J. Efficacy of the antimicrobial peptide TP4 againstHelicobacter pylori infection:in vitro membrane perturbationvia micellization andin vivo suppression of host immune responses in a mouse model. Oncotarget. 2015;6(15):12936-54.
14. Yi HB, Zhang L, Gan ZS, Xiong HT, Yu C, Du H, et al. High therapeutic efficacy of Cathelicidin-WA against postweaning diarrhea via inhibiting inflammation and enhancing epithelial barrier in the intestine. Sci Rep-Uk. 2016;6(1):25679.
15. Wang L, Zhao X, Zhu C, Xia X, Qin W, Li M, et al. Thymol kills bacteria, reduces biofilm formation, and protects mice against a fatal infection of Actinobacillus pleuropneumoniae strain L20. Vet Microbiol. 2017;203:202-210.
16. Zhang L, Wei X, Zhang R, Petitte JN, Si D, Li Z, et al. Design and development of a novel peptide for treating intestinal inflammation. Front Immunol. 2019;10:1841.
17. Chromek M, Arvidsson I, Karpman D, Bereswill S. The Antimicrobial Peptide Cathelicidin Protects Mice from Escherichia coli O157:H7-Mediated Disease. Plos One. 2012;7(10):e46476.
18. Ribes S, Arcilla C, Ott M, Schütze S, Hanisch U, Nessler S, et al. Pre-treatment with the viral Toll-like receptor 3 agonist poly(I:C) modulates innate immunity and protects neutropenic mice infected intracerebrally with Escherichia coli. J Neuroinflamm. 2020;17(1):24.

19. Millot P, San C, Bennana E, Porte B, Vignal N, Hugon J, et al. STAT3 inhibition protects against neuroinflammation and BACE1 upregulation induced by systemic inflammation. Immunol Lett. 2020;S0165-2478(20):30400-4.
20. Martens K, Seys SF, Alpizar YA, Schrijvers R, Bullens DMA, Breynaert C, et al. Staphylococcus aureus enterotoxin B disrupts nasal epithelial barrier integrity. Clinical & Experimental Allergy. 2020; doi: 10.1111/cea.13760.
21. Malecki C, Hambly BD, Jeremy RW, Robertson EN. The role of inflammation and Myeloperoxidase-Related oxidative stress in the pathogenesis of genetically triggered thoracic aortic aneurysms. Int J Mol Sci. 2020;21(20):7678.
22. Wang L, Zhao X, Xia X, Zhu C, Zhang H, Qin W, et al. Inhibitory Effects of Antimicrobial Peptide JH-3 on Salmonella enterica Serovar Typhimurium Strain CVCC541 Infection-Induced Inflammatory Cytokine Release and Apoptosis in RAW264.7 Cells. Molecules. 2019;24(3):596.
23. Lutz TM, Marczynski M, Grill MJ, Wall WA, Lieleg O. Repulsive backbone–backbone interactions modulate access to specific and unspecific binding sites on Surface-Bound mucins. Langmuir. 2020;36(43):12973-82.
24. Mahlapuu M, Håkansson J, Ringstad L, Björn C, Sahlgrenska A, Institute Of Medicine DOMA, et al. Antimicrobial peptides: An emerging category of therapeutic agents. Front Cell Infect Mi. 2016;6:194.
25. Csernus B, Czeglédi L. Physiological, antimicrobial, intestine morphological, and immunological effects of fructooligosaccharides in pigs. Arch Anim Breed. 2020;63(2):325-35.
26. Daneshmand A, Kermanshahi H, Sekhavati MH, Javadmanesh A, Ahmadian M, Alizadeh M, et al. Effects of cLFchimera peptide on intestinal morphology, integrity, microbiota, and immune cells in broiler chickens challenged with necrotic enteritis. Sci Rep. 2020;10(1):17704.
27. Liang X, Zhang X, Lian K, Tian X, Zhang M, Wang S, et al. Antiviral effects of Bovine antimicrobial peptide against TGEV in vivo and in vitro. Journal of veterinary science (Suwŏn-si, Korea). 2020;21(5):e80.
28. Wang L, Zhao X, Xia X, Zhu C, Qin W, Xu Y, et al. Antimicrobial peptide JH-3 effectively kills salmonella enterica serovar typhimurium strain CVCC541 and reduces its pathogenicity in mice. Probiotics Antimicrob Proteins. 2019;11(4):1379-90.
29. Wang G. Bioinformatic analysis of 1000 amphibian antimicrobial peptides uncovers multiple Length-Dependent correlations for peptide design and prediction. Antibiotics. 2020;9(8):491.
30. Lee SH, Lillehoj HS, Jang SI, Lillehoj EP, Min W, Bravo DM. Dietary supplementation of young broiler chickens with Capsicum and turmeric oleoresins increases resistance to necrotic enteritis. Brit J Nutr. 2013;110(5):840-7.
31. Wubulikasimu A, Huang Y, Wali A, Yili A, Rong M. A designed antifungal peptide with therapeutic potential for clinical drug-resistant Candida albicans. Biochem Bioph Res Co. 2020;533(3):404-9.
32. Shin MK, Hwang I, Kim Y, Kim ST, Jang W, Lee S, et al. Antibacterial and Anti-Inflammatory Effects of Novel Peptide Toxin from the Spider Pardosa astrigera. Antibiotics (Basel). 2020;9(7):422.

33. Han F, Zhang H, Xia X, Xiong H, Song D, Zong X, et al. Porcine β-Defensin 2 attenuates inflammation and mucosal lesions in dextran sodium sulfate–induced colitis. The Journal of Immunology. 2015;194(4):1882-93.
34. Huang Z, Liu J, Ong HH, Yuan T, Zhou X, Wang J, et al. Interleukin-13 alters tight junction proteins expression thereby compromising barrier function and dampens rhinovirus induced immune responses in nasal epithelium. Frontiers in cell and developmental biology. 2020;8:572749.
35. Lin Q, Su G, Wu A, Chen D, Yu B, Huang Z, et al. Bombyx mori gloverin A2 alleviates enterotoxigenic Escherichia coli-induced inflammation and intestinal mucosa disruption. Antimicrobial Resistance & Infection Control. 2019;8(1):189.
36. Zhang LL, Wei XB, Zhang R, Petitte JN, Si D, Li Z, et al. Design and development of a novel peptide for treating intestinal inflammation. Front Immunol. 2019;10:1841.
37. Yu H, Wang Y, Zeng X, Cai S, Wang G, Liu L, et al. Therapeutic administration of the recombinant antimicrobial peptide microcin J25 effectively enhances host defenses against gut inflammation and epithelial barrier injury induced by enterotoxigenic Escherichia coli infection. The FASEB journal. 2020;34(1):1018-37.

Figures

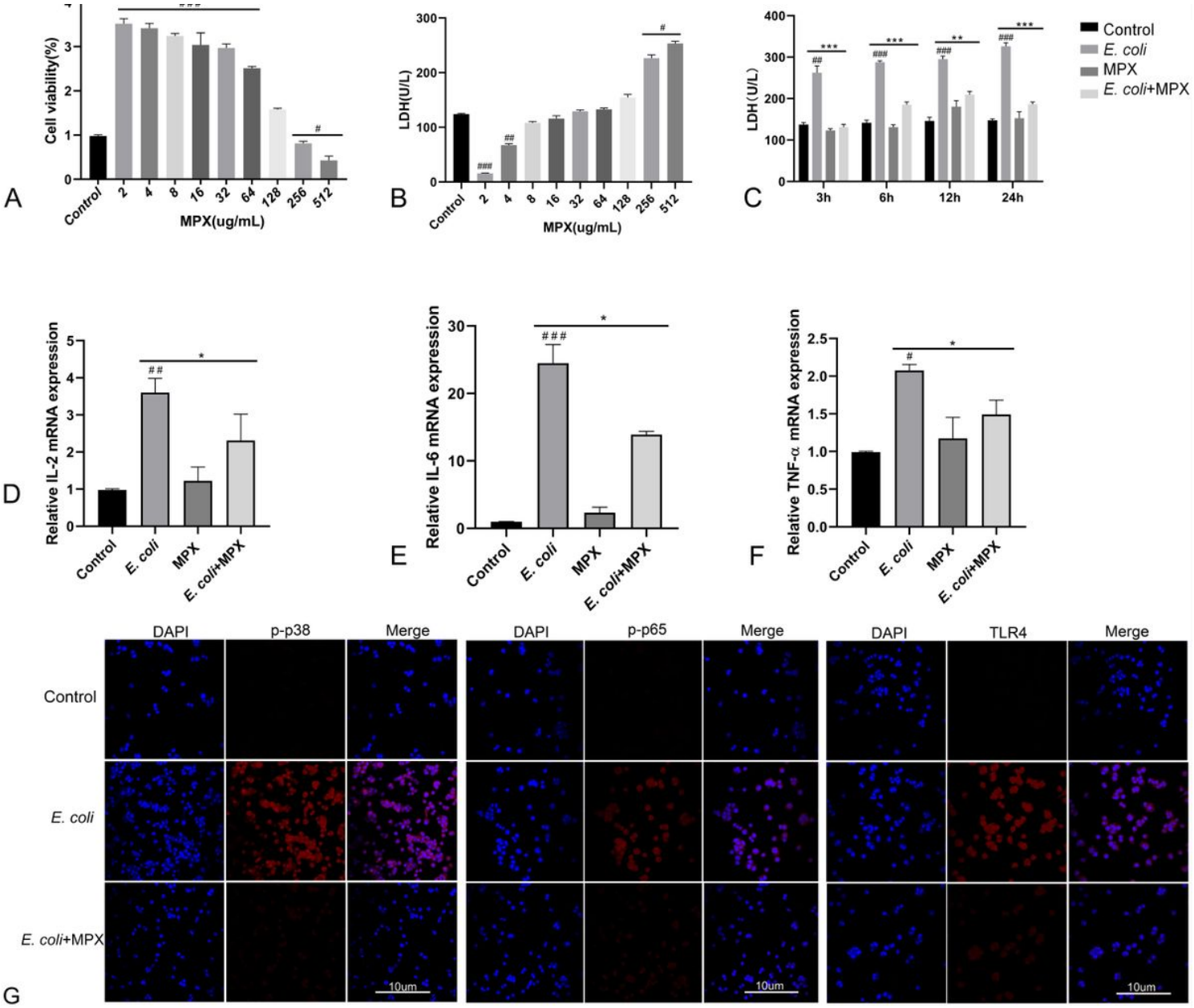

Figure 1

MPX does not induce cytotoxicity and alleviates inflammation in IPEC-J2 cells. (a) Cell viability was measured using the CCK-8 assay, IPEC-J2 cells were cultured with different concentrations (2-512 μg/mL) of MPX for 24 h; (b) The release of LDH from IPEC-J2 cells after treatment with different concentrations (2-512 μg/mL) of MPX for 24 h; (c) MPX decreased the E. coli-induced release of LDH from IPEC-J2 cells (MOI=10) at different times; (d-f) The mRNA expression of IL-2, IL-6 and TNF-α after MPX treatment. (g) The expression of p-p38, p-p65 and TLR4 in IPEC-J2 cells assessed by confocal laser microscopy. #P < 0.05; ##P < 0.01; ###P < 0.001 E. coli vs control; *P < 0.05;**P < 0.01; ***P < 0.001 MPX treatment vs E. coli.

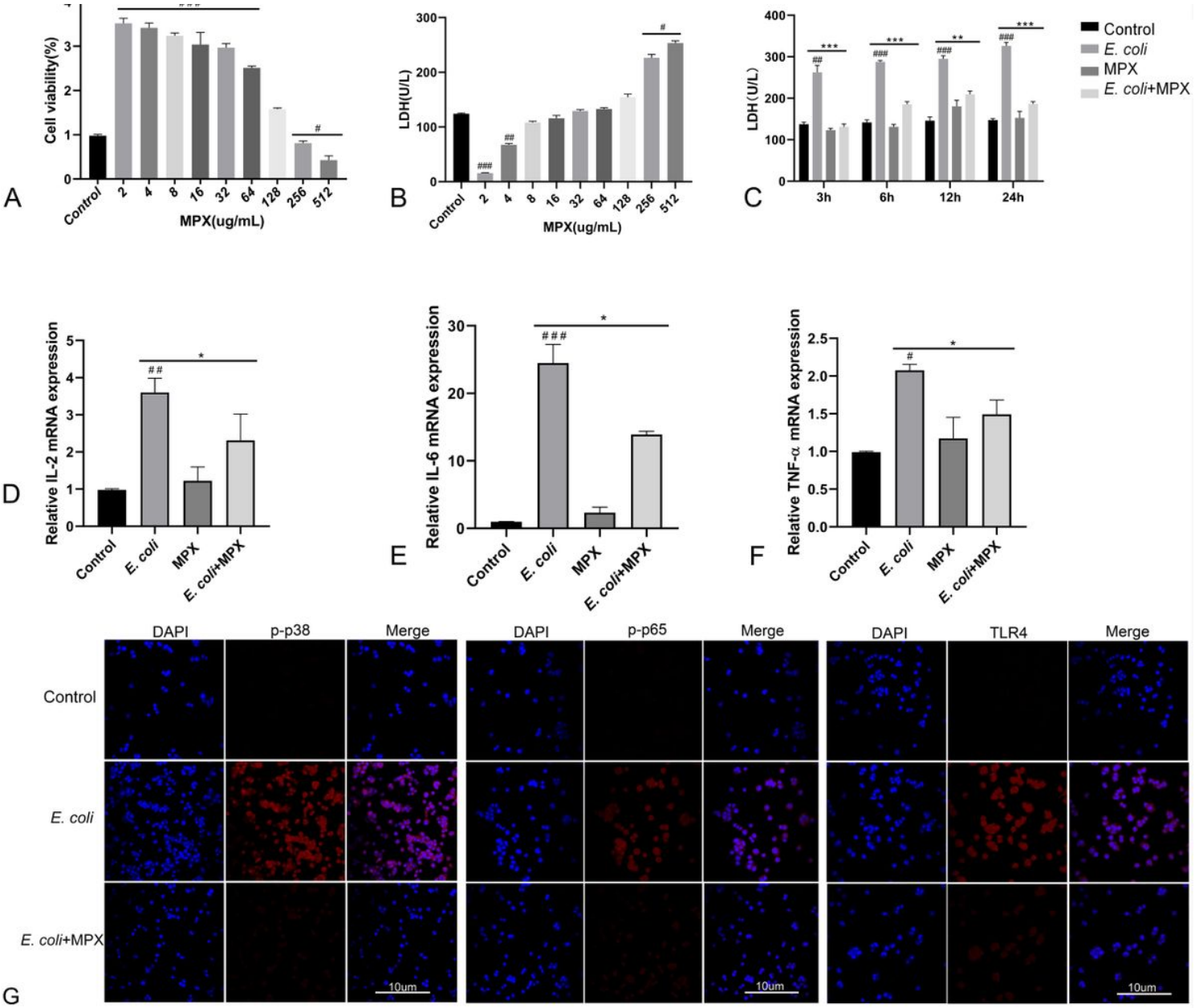

Figure 1

MPX does not induce cytotoxicity and alleviates inflammation in IPEC-J2 cells. (a) Cell viability was measured using the CCK-8 assay, IPEC-J2 cells were cultured with different concentrations (2-512 μg/mL) of MPX for 24 h; (b) The release of LDH from IPEC-J2 cells after treatment with different concentrations (2-512 μg/mL) of MPX for 24 h; (c) MPX decreased the E. coli-induced release of LDH from IPEC-J2 cells (MOI=10) at different times; (d-f) The mRNA expression of IL-2, IL-6 and TNF-α after MPX treatment. (g) The expression of p-p38, p-p65 and TLR4 in IPEC-J2 cells assessed by confocal laser microscopy. #P < 0.05; ##P < 0.01; ###P < 0.001 E. coli vs control; *P < 0.05;**P < 0.01; ***P < 0.001 MPX treatment vs E. coli.

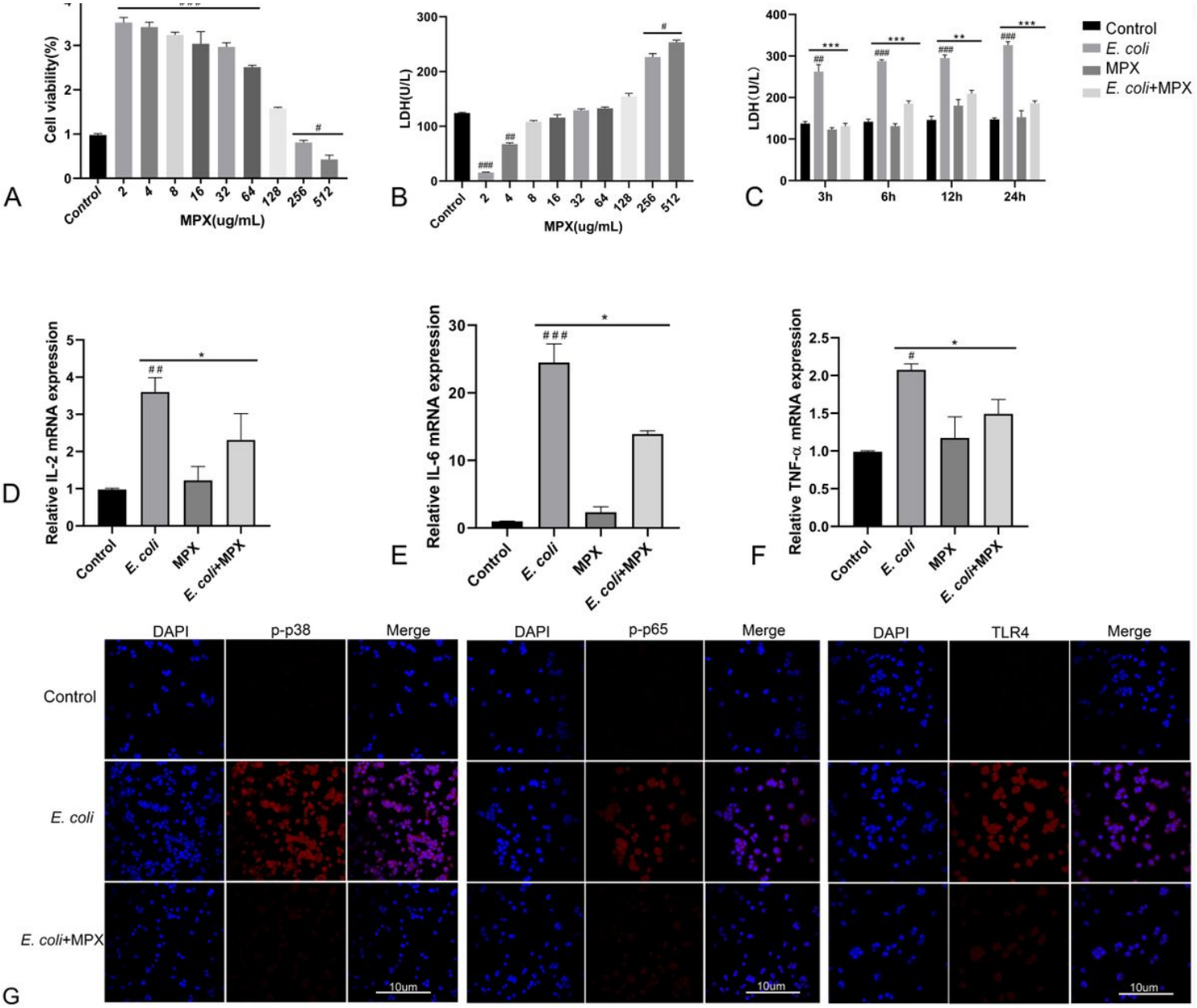

Figure 1

MPX does not induce cytotoxicity and alleviates inflammation in IPEC-J2 cells. (a) Cell viability was measured using the CCK-8 assay, IPEC-J2 cells were cultured with different concentrations (2-512 μg/mL) of MPX for 24 h; (b) The release of LDH from IPEC-J2 cells after treatment with different concentrations (2-512 μg/mL) of MPX for 24 h; (c) MPX decreased the E. coli-induced release of LDH from IPEC-J2 cells (MOI=10) at different times; (d-f) The mRNA expression of IL-2, IL-6 and TNF-α after MPX treatment. (g) The expression of p-p38, p-p65 and TLR4 in IPEC-J2 cells assessed by confocal laser microscopy. #P < 0.05; ##P < 0.01; ###P < 0.001 E. coli vs control; *P < 0.05;**P < 0.01; ***P < 0.001 MPX treatment vs E. coli.

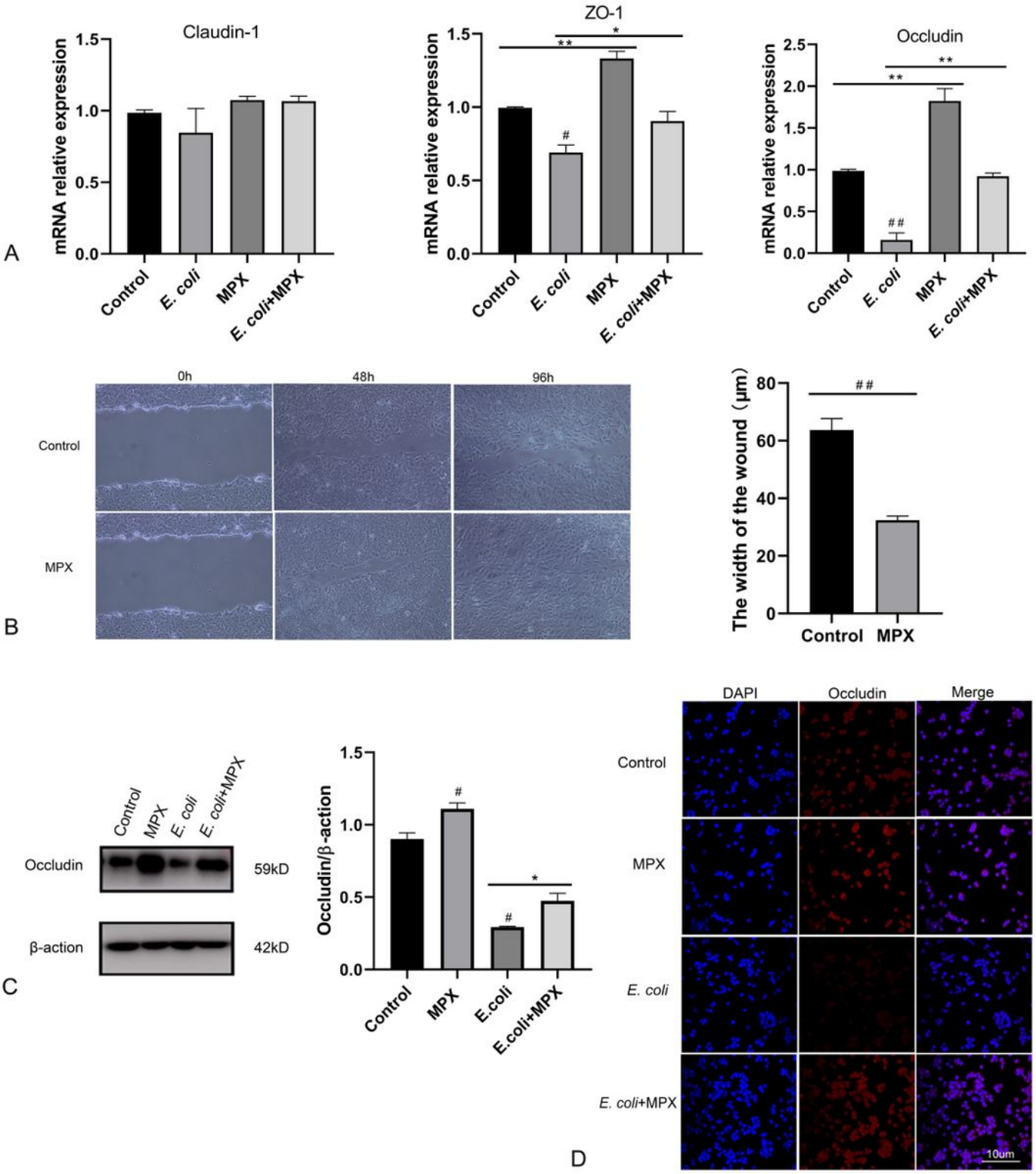

Figure 2

MPX enhances IPEC-J2 cell barrier function. (a) The E. coli-induced mRNA expression of ZO-1, occludin and claudin-1 in IPEC-J2 cells after treatment with MPX; (b) IPEC-J2 cells were incubated with medium alone or MPX (10 μg/mL) in a wound healing assay. Images were obtained at 0 h, 48 h and 96 h, and the wound width was measured at 48 h; (c) The E. coli-induced protein level of occludin in IPEC-J2 cells after pretreatment with MPX was determined by western blotting; (d) The effect of MPX on the expression of

occludin in IPEC-J2 cells was assessed by confocal laser microscopy. #P < 0.05; ##P < 0.01; ###P < 0.001 E. coli vs control; *P < 0.05;**P < 0.01; ***P < 0.001 MPX treatment vs E.coli.

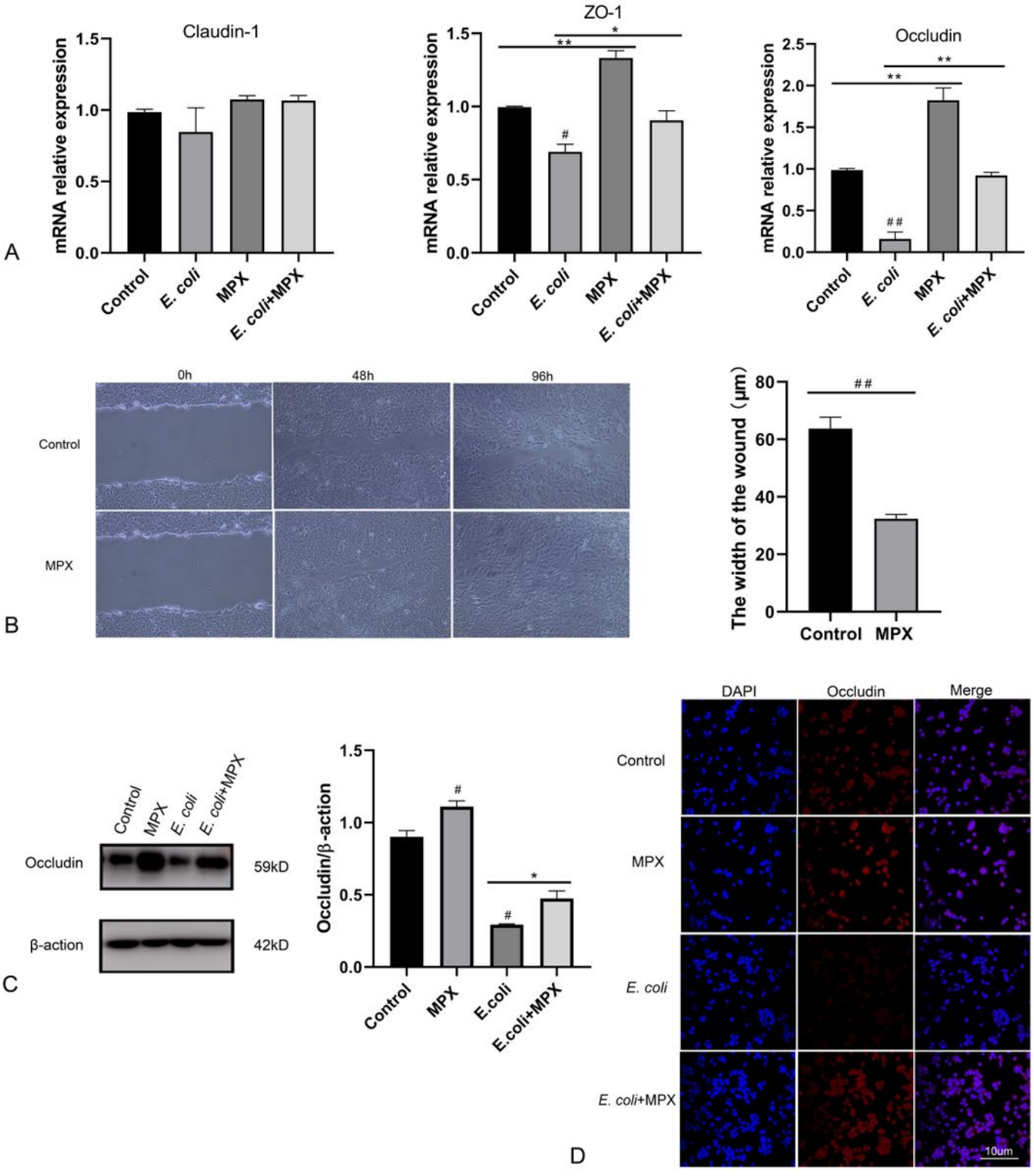

Figure 2

MPX enhances IPEC-J2 cell barrier function. (a) The E. coli-induced mRNA expression of ZO-1, occludin and claudin-1 in IPEC-J2 cells after treatment with MPX; (b) IPEC-J2 cells were incubated with medium alone or MPX (10 μg/mL) in a wound healing assay. Images were obtained at 0 h, 48 h and 96 h, and the

wound width was measured at 48 h; (c) The E. coli-induced protein level of occludin in IPEC-J2 cells after pretreatment with MPX was determined by western blotting; (d) The effect of MPX on the expression of occludin in IPEC-J2 cells was assessed by confocal laser microscopy. #P < 0.05; ##P < 0.01; ###P < 0.001 E. coli vs control; *P < 0.05;**P < 0.01; ***P < 0.001 MPX treatment vs E.coli.

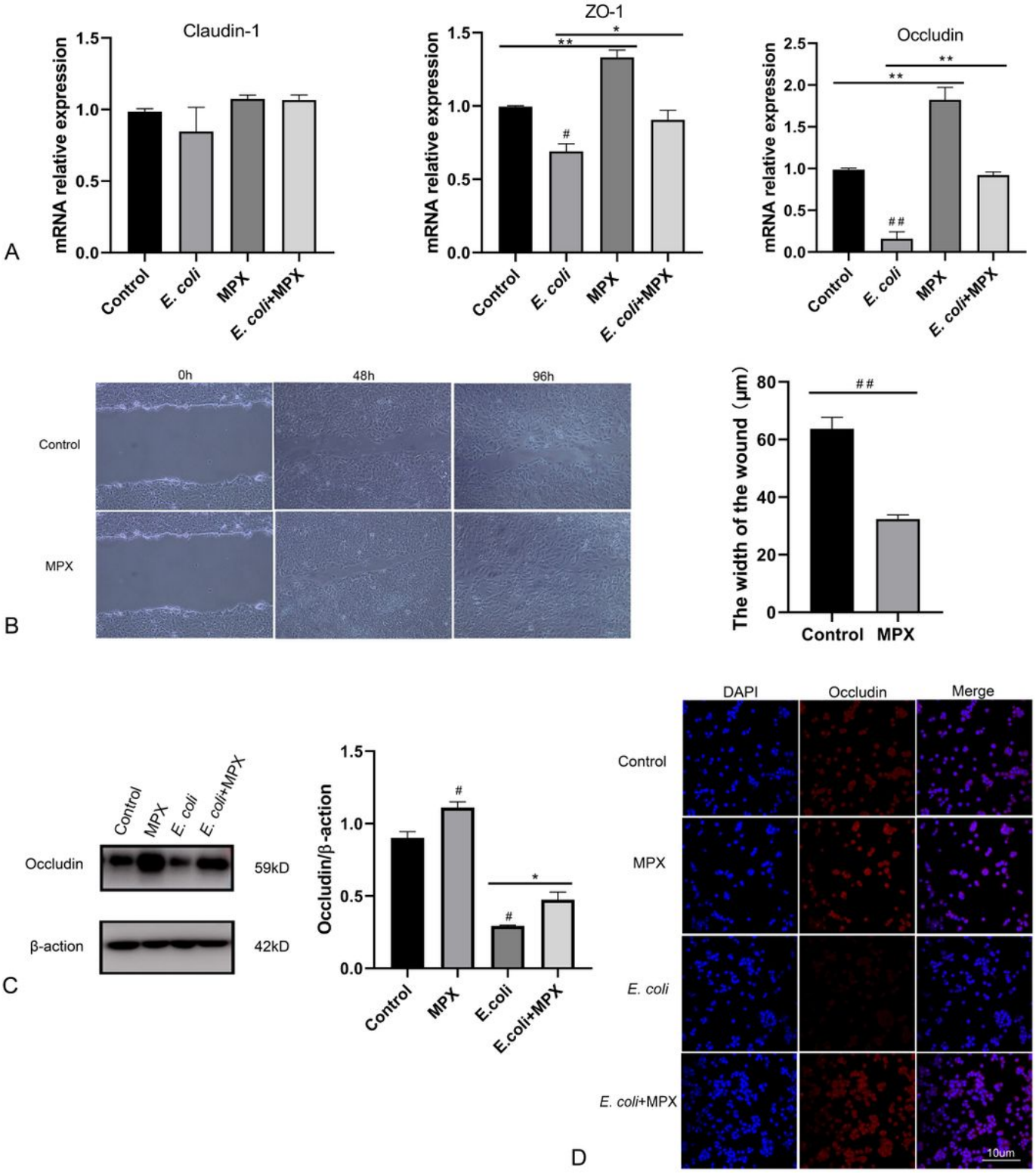

Figure 2

MPX enhances IPEC-J2 cell barrier function. (a) The E. coli-induced mRNA expression of ZO-1, occludin and claudin-1 in IPEC-J2 cells after treatment with MPX; (b) IPEC-J2 cells were incubated with medium alone or MPX (10 μg/mL) in a wound healing assay. Images were obtained at 0 h, 48 h and 96 h, and the wound width was measured at 48 h; (c) The E. coli-induced protein level of occludin in IPEC-J2 cells after pretreatment with MPX was determined by western blotting; (d) The effect of MPX on the expression of occludin in IPEC-J2 cells was assessed by confocal laser microscopy. #P < 0.05; ##P < 0.01; ###P < 0.001 E. coli vs control; *P < 0.05;**P < 0.01; ***P < 0.001 MPX treatment vs E.coli.

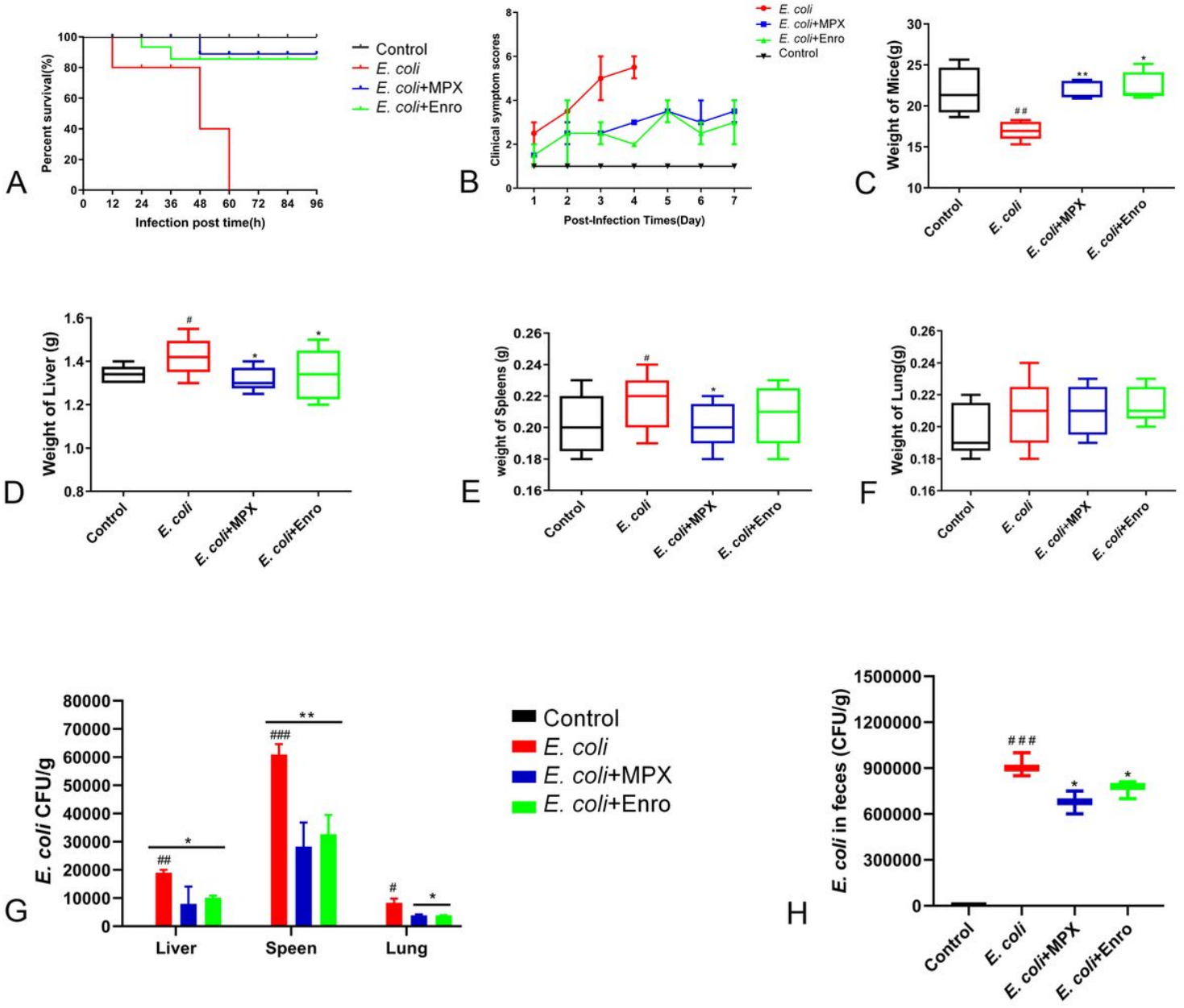

Figure 3

MPX protects mice against infection with a lethal dose of E. coli. (a) The survival rate of mice infected with E. coli after MPX treatment; (b) The clinical symptom score of mice infected with E. coli after MPX treatment; (c) The weight of mice infected with E. coli after MPX treatment; (d-f) The weight of the liver, spleen and lung of mice infected with E. coli after MPX treatment; (g) The number of bacteria in the liver,

spleen and lung of mice infected with E. coli after MPX treatment; (h) The number of bacteria in the feces of mice infected with E. coli after MPX treatment. Control group, mice injected with sterile saline; E. coli group, mice injected with E. coli; MPX group, mice treated with intraperitoneal injection MPX and injected with E. coli. #P < 0.05; ##P < 0.01; ###P < 0.001 E. coli vs control; *P < 0.05;**P < 0.01; ***P < 0.001 MPX and Enro treatment vs E. coli.

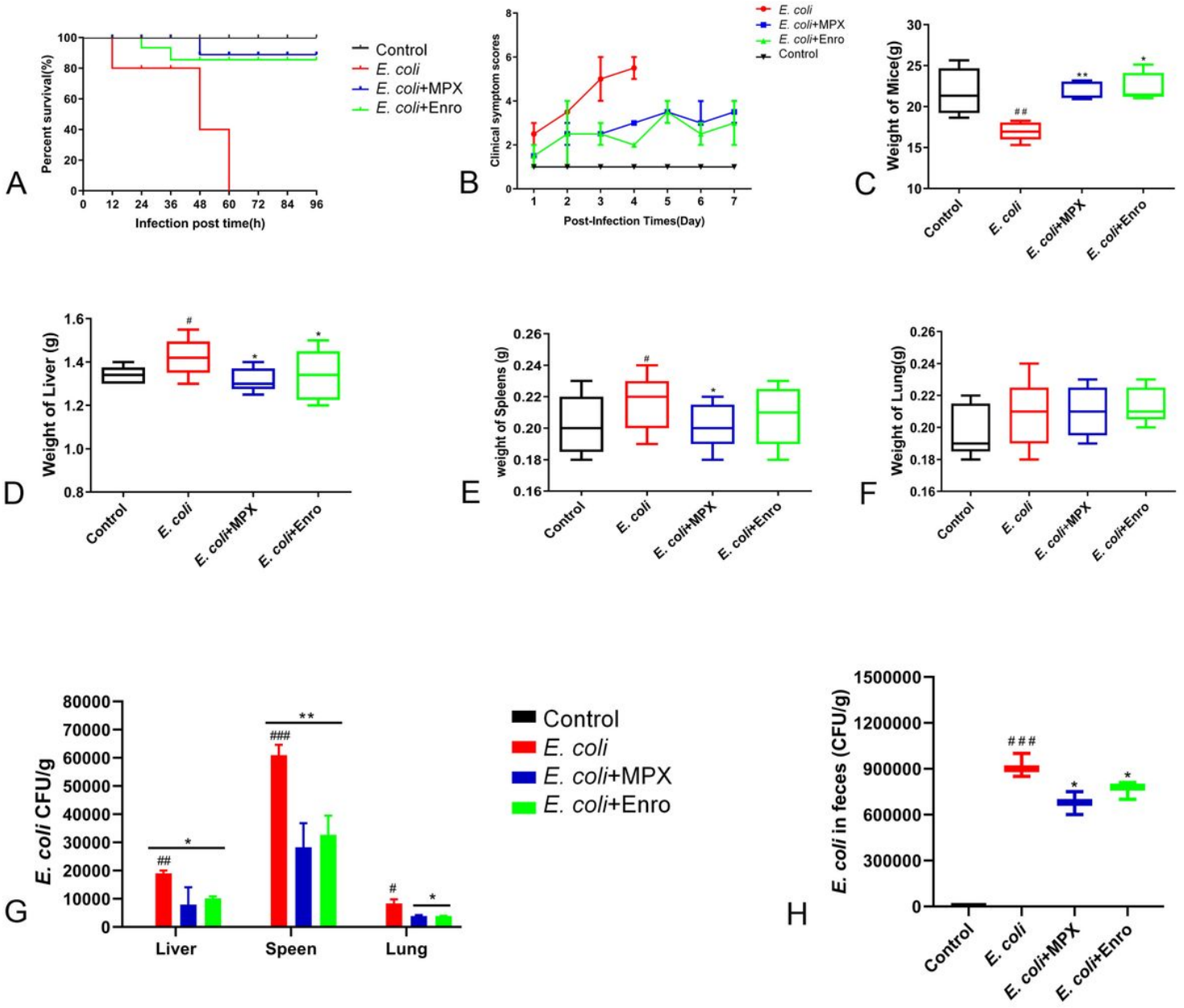

Figure 3

MPX protects mice against infection with a lethal dose of E. coli. (a) The survival rate of mice infected with E. coli after MPX treatment; (b) The clinical symptom score of mice infected with E. coli after MPX treatment; (c) The weight of mice infected with E. coli after MPX treatment; (d-f) The weight of the liver, spleen and lung of mice infected with E. coli after MPX treatment; (g) The number of bacteria in the liver, spleen and lung of mice infected with E. coli after MPX treatment; (h) The number of bacteria in the feces of mice infected with E. coli after MPX treatment. Control group, mice injected with sterile saline; E. coli

group, mice injected with E. coli; MPX group, mice treated with intraperitoneal injection MPX and injected with E. coli. #P < 0.05; ##P < 0.01; ###P < 0.001 E. coli vs control; *P < 0.05;**P < 0.01; ***P < 0.001 MPX and Enro treatment vs E. coli.

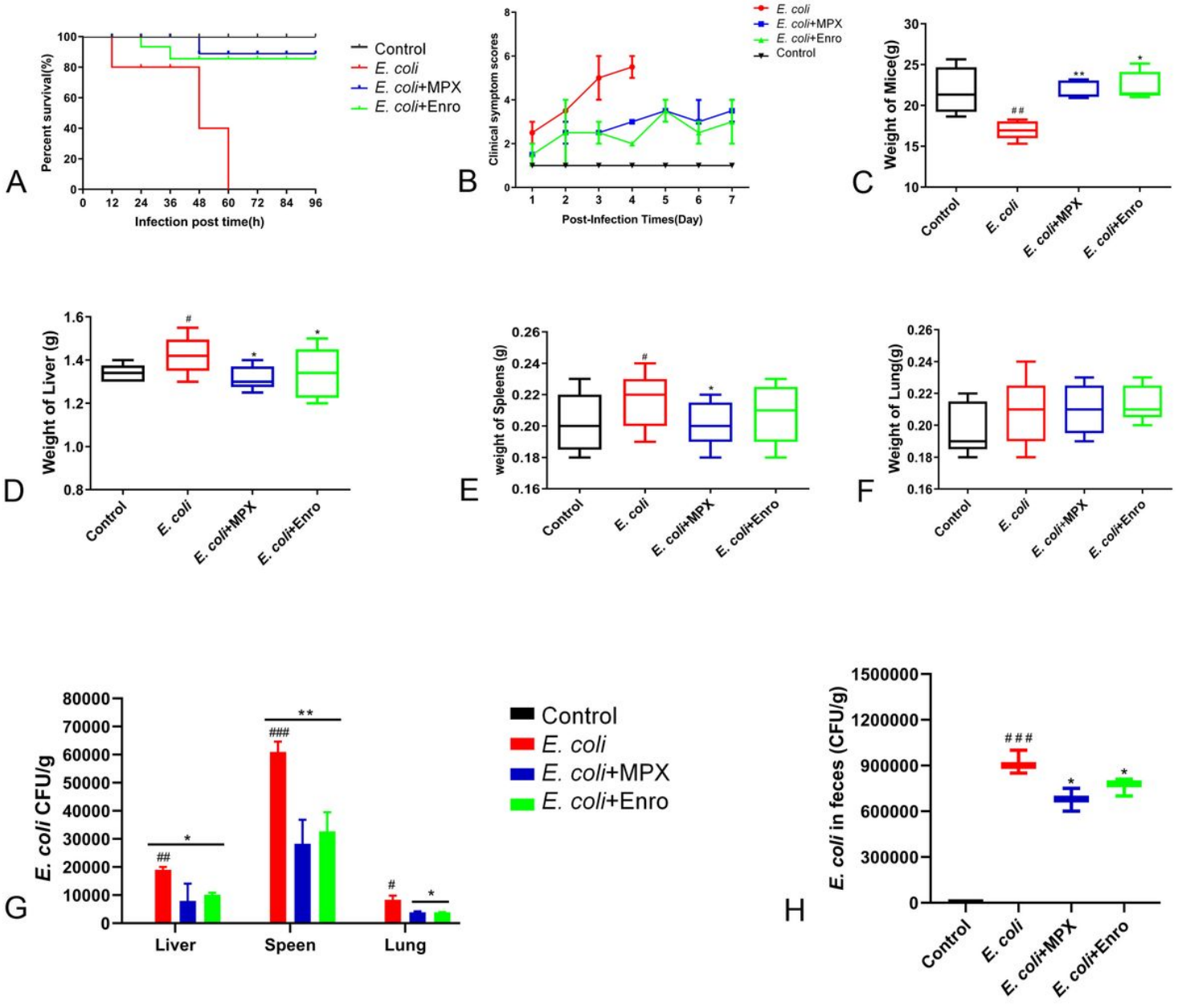

Figure 3

MPX protects mice against infection with a lethal dose of E. coli. (a) The survival rate of mice infected with E. coli after MPX treatment; (b) The clinical symptom score of mice infected with E. coli after MPX treatment; (c) The weight of mice infected with E. coli after MPX treatment; (d-f) The weight of the liver, spleen and lung of mice infected with E. coli after MPX treatment; (g) The number of bacteria in the liver, spleen and lung of mice infected with E. coli after MPX treatment; (h) The number of bacteria in the feces of mice infected with E. coli after MPX treatment. Control group, mice injected with sterile saline; E. coli group, mice injected with E. coli; MPX group, mice treated with intraperitoneal injection MPX and injected

with E. coli. #P < 0.05; ##P < 0.01; ###P < 0.001 E. coli vs control; *P < 0.05;**P < 0.01; ***P < 0.001 MPX and Enro treatment vs E. coli.

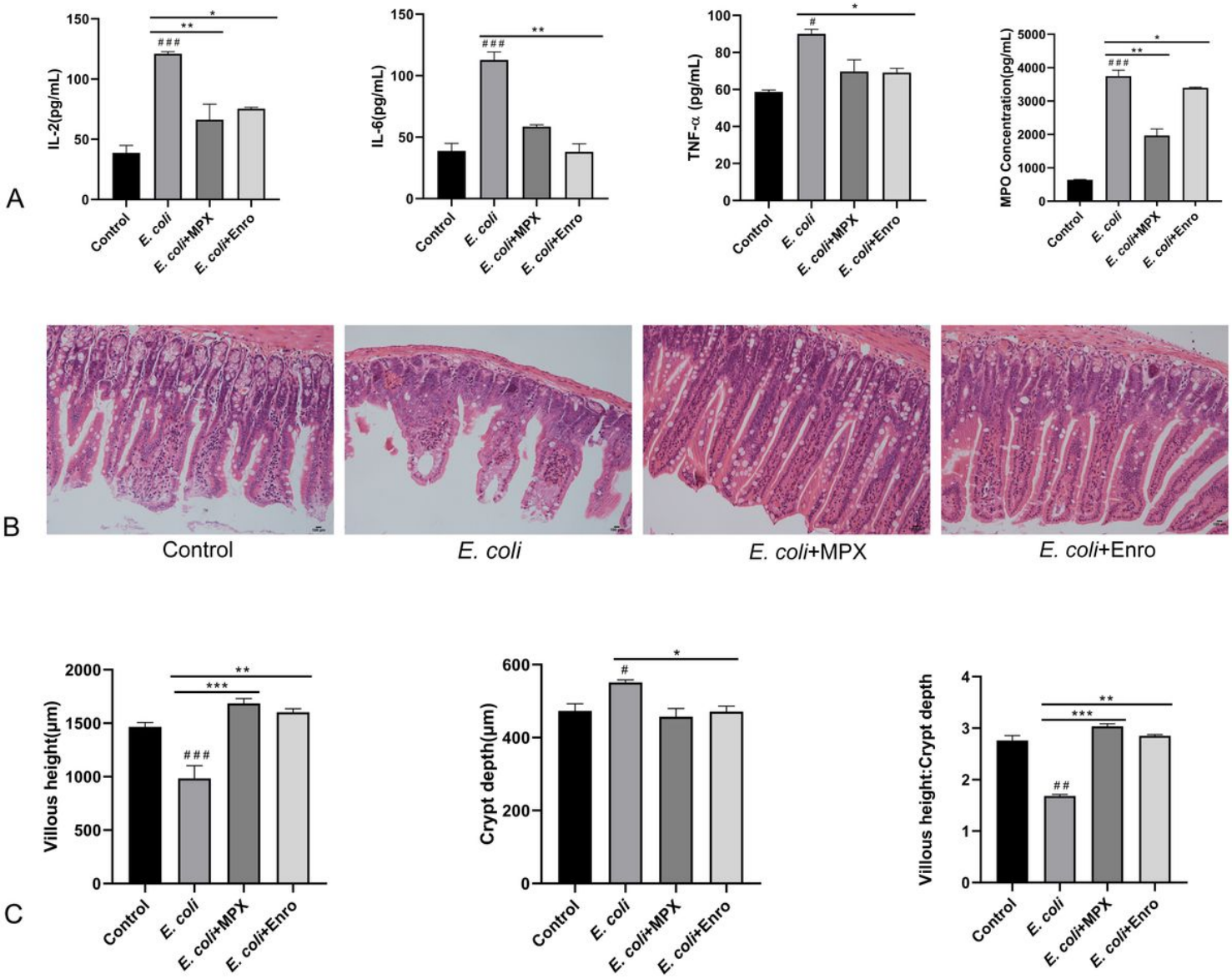

Figure 4

MPX inhibits inflammatory cytokine expression and improves intestinal morphology. (a) The levels of inflammatory cytokines (IL-2, IL-6 and TNF-α) and MPO in mouse serum were detected using ELISA; (b) The jejunum of mice was stained with H&E (bars, 100 μm); images were obtained at 200× magnification; (c) The length of jejunal villi, the depth of crypts, and the ratios of villi length to crypt depth were detected by ipwin32 software. #P < 0.05; ##P < 0.01; ###P < 0.001 E. coli vs control; *P < 0.05; **P < 0.01; ***P < 0.001 MPX and Enro treatment vs E. coli.

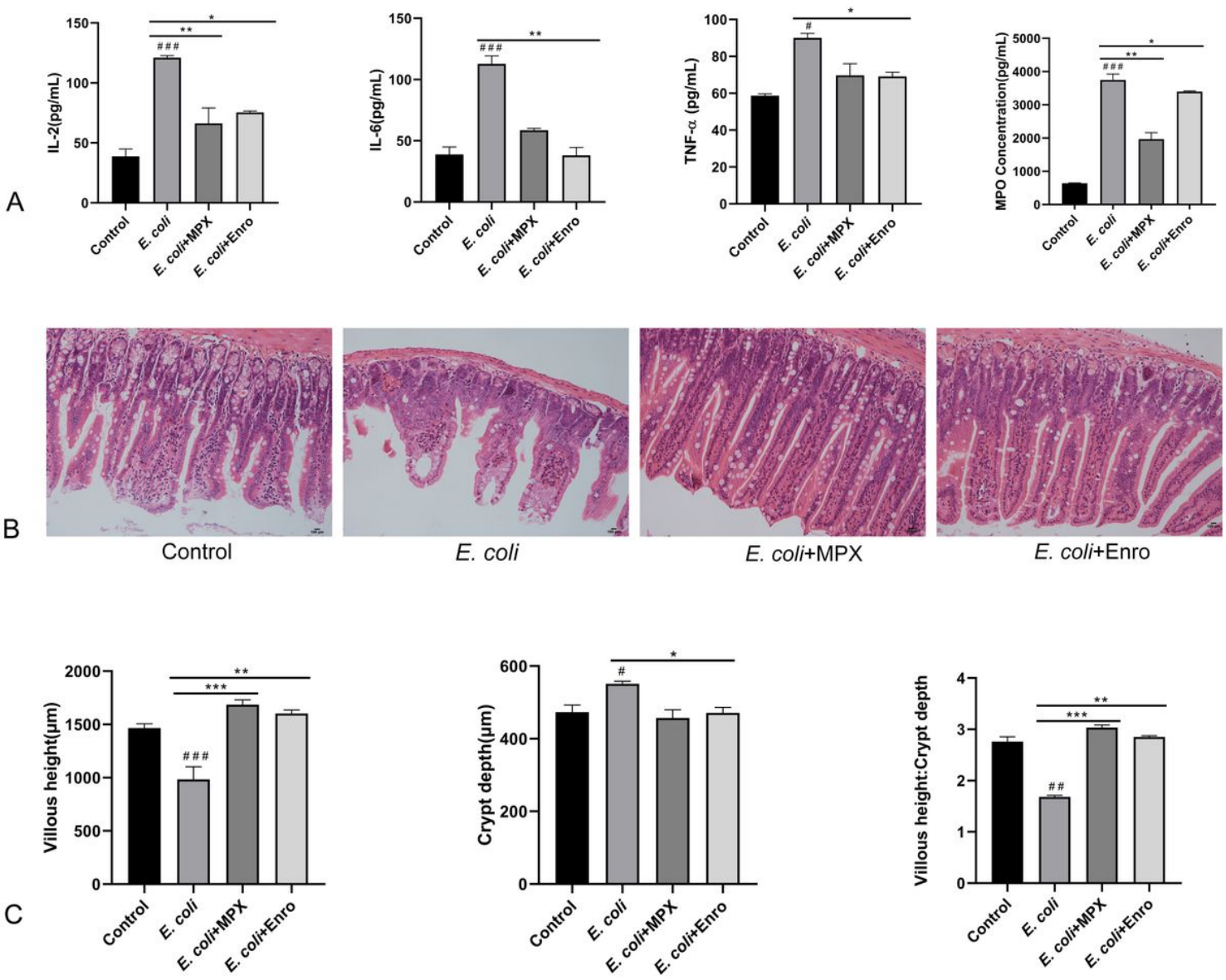

Figure 4

MPX inhibits inflammatory cytokine expression and improves intestinal morphology. (a) The levels of inflammatory cytokines (IL-2, IL-6 and TNF-α) and MPO in mouse serum were detected using ELISA; (b) The jejunum of mice was stained with H&E (bars, 100 μm); images were obtained at 200× magnification; (c) The length of jejunal villi, the depth of crypts, and the ratios of villi length to crypt depth were detected by ipwin32 software. #P < 0.05; ##P < 0.01; ###P < 0.001 E. coli vs control; *P < 0.05; **P < 0.01; ***P < 0.001 MPX and Enro treatment vs E. coli.

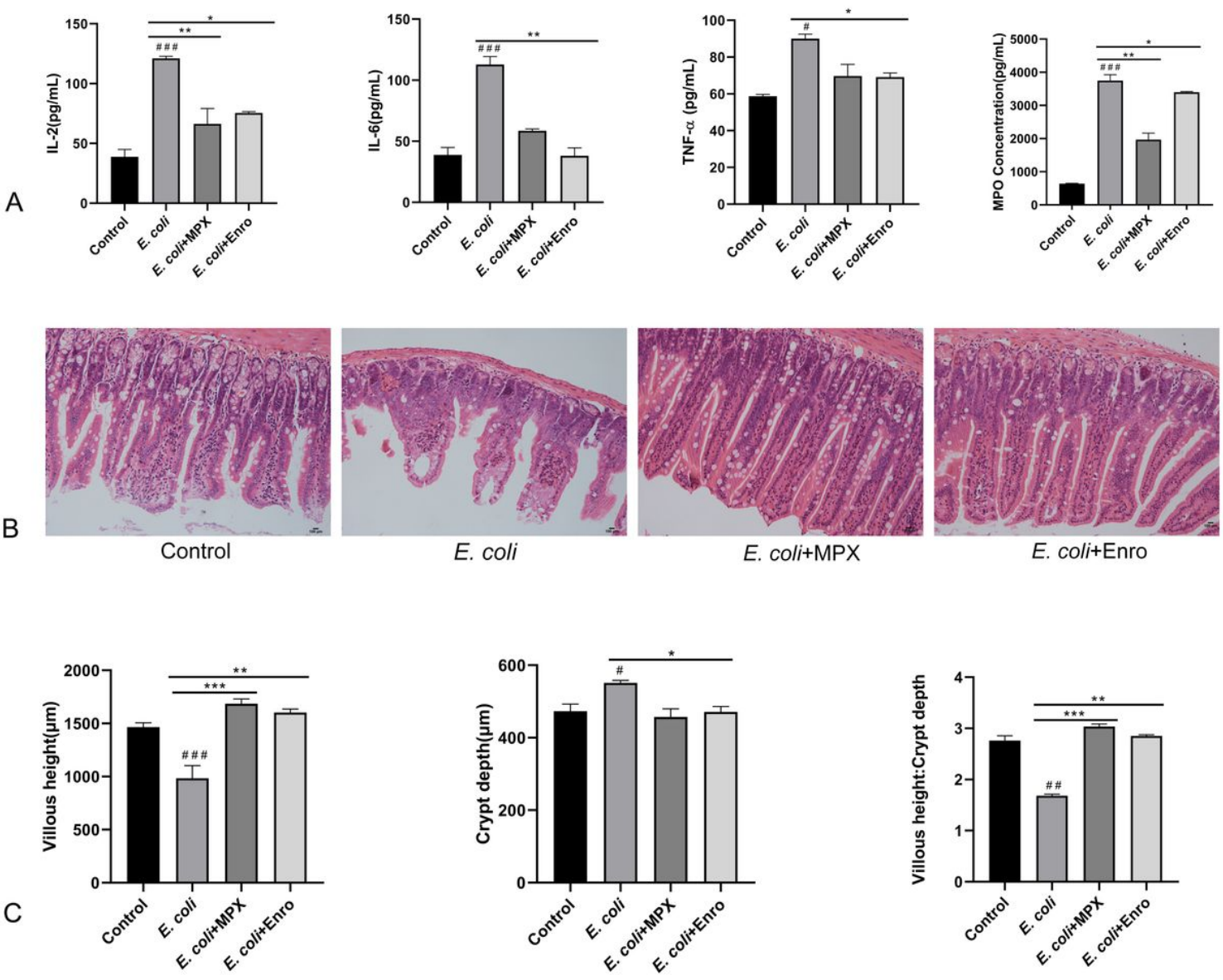

Figure 4

MPX inhibits inflammatory cytokine expression and improves intestinal morphology. (a) The levels of inflammatory cytokines (IL-2, IL-6 and TNF-α) and MPO in mouse serum were detected using ELISA; (b) The jejunum of mice was stained with H&E (bars, 100 μm); images were obtained at 200× magnification; (c) The length of jejunal villi, the depth of crypts, and the ratios of villi length to crypt depth were detected by ipwin32 software. #P < 0.05; ##P < 0.01; ###P < 0.001 E. coli vs control; *P < 0.05; **P < 0.01; ***P < 0.001 MPX and Enro treatment vs E. coli.

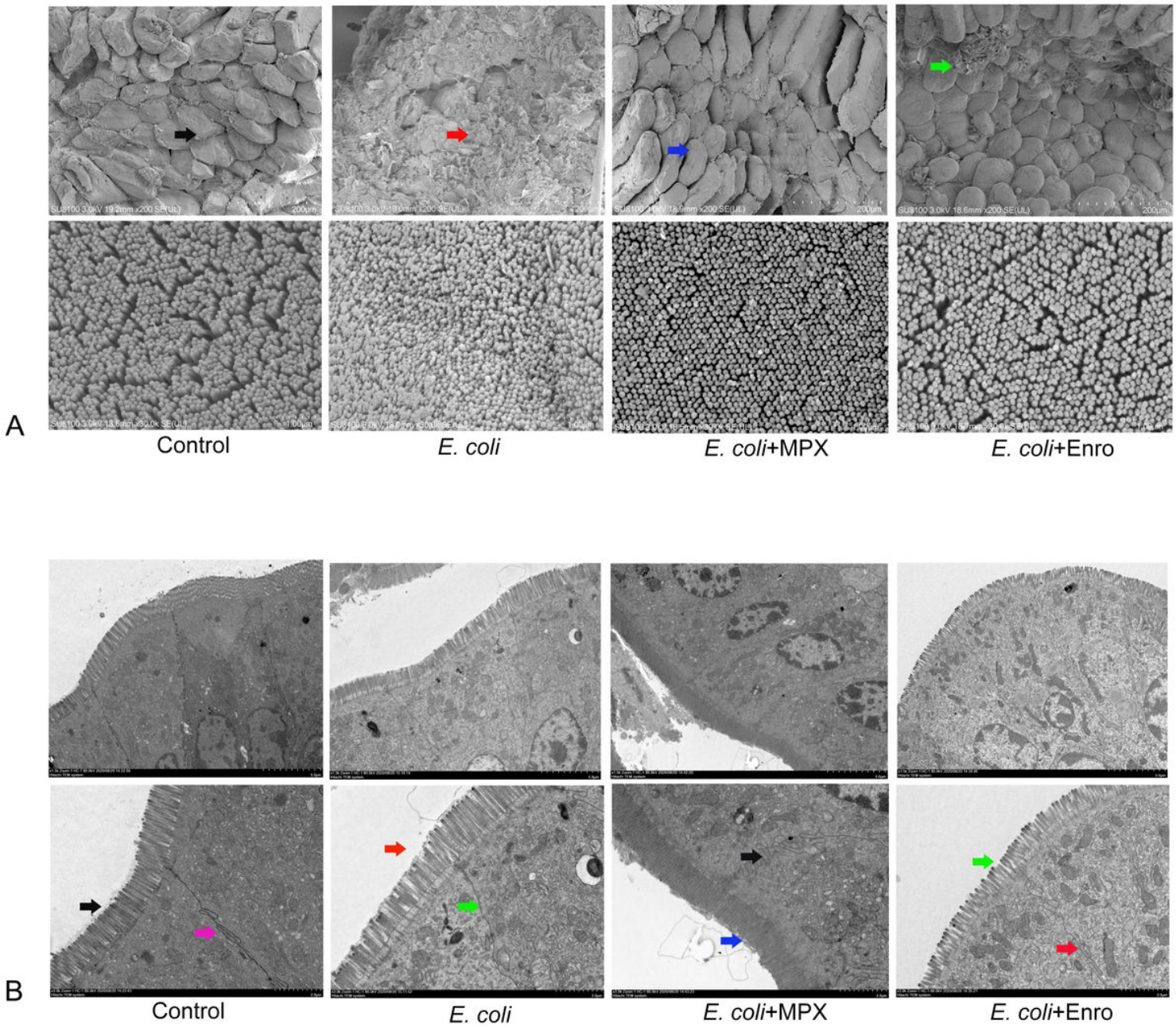

Figure 5

MPX improves the intestinal morphology of the jejunum and the microvilli of intestinal epithelial cells. (a) Morphological changes in the jejunum villi were observed by SEM (upper, 200×; lower, 30,000×); (b) Morphological changes in the microvilli and tight junction proteins in intestinal epithelial cells were observed by TEM (upper, 1500×; lower, 3000×).

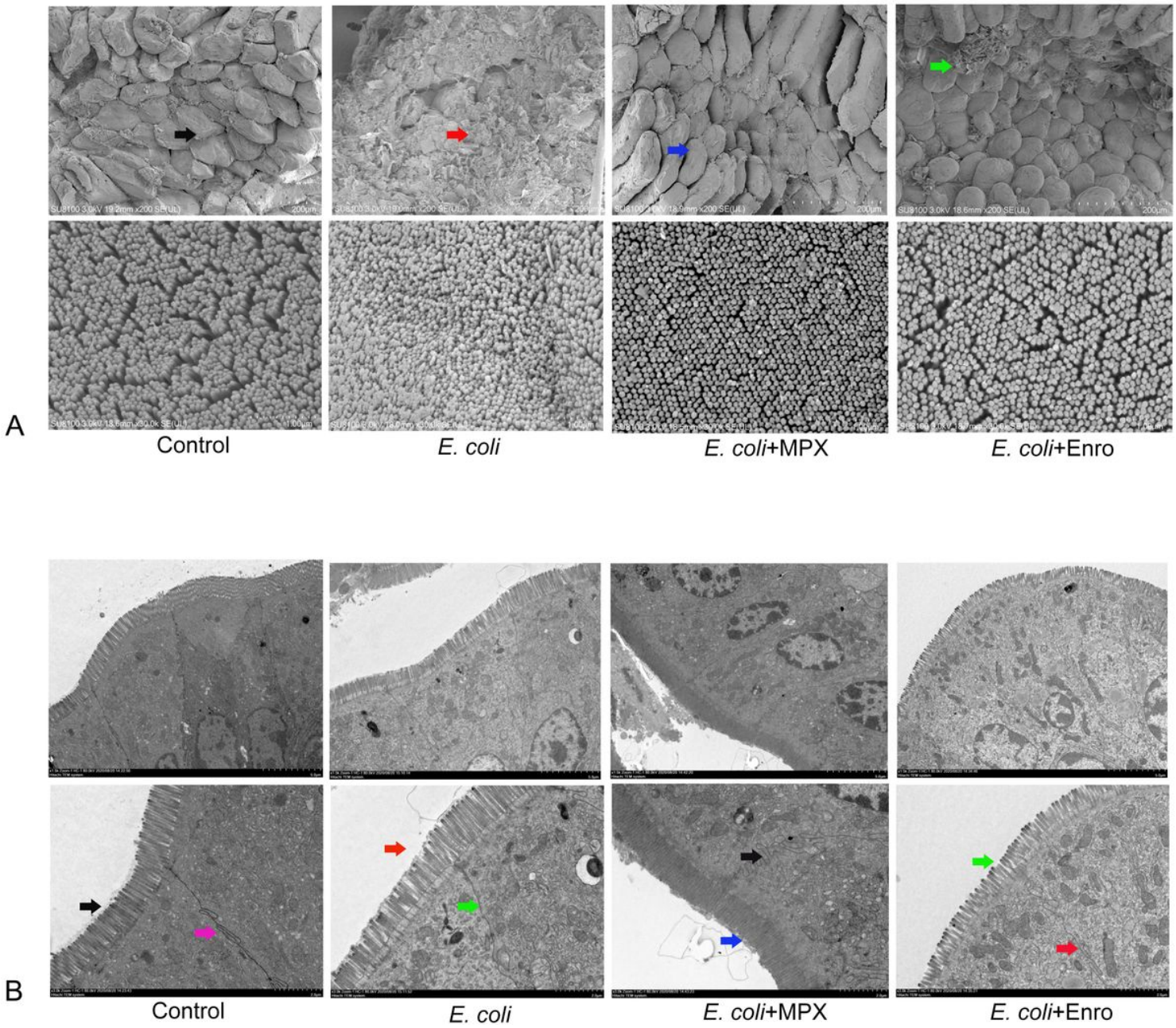

Figure 5

MPX improves the intestinal morphology of the jejunum and the microvilli of intestinal epithelial cells. (a) Morphological changes in the jejunum villi were observed by SEM (upper, 200×; lower, 30,000×); (b) Morphological changes in the microvilli and tight junction proteins in intestinal epithelial cells were observed by TEM (upper, 1500×; lower, 3000×).

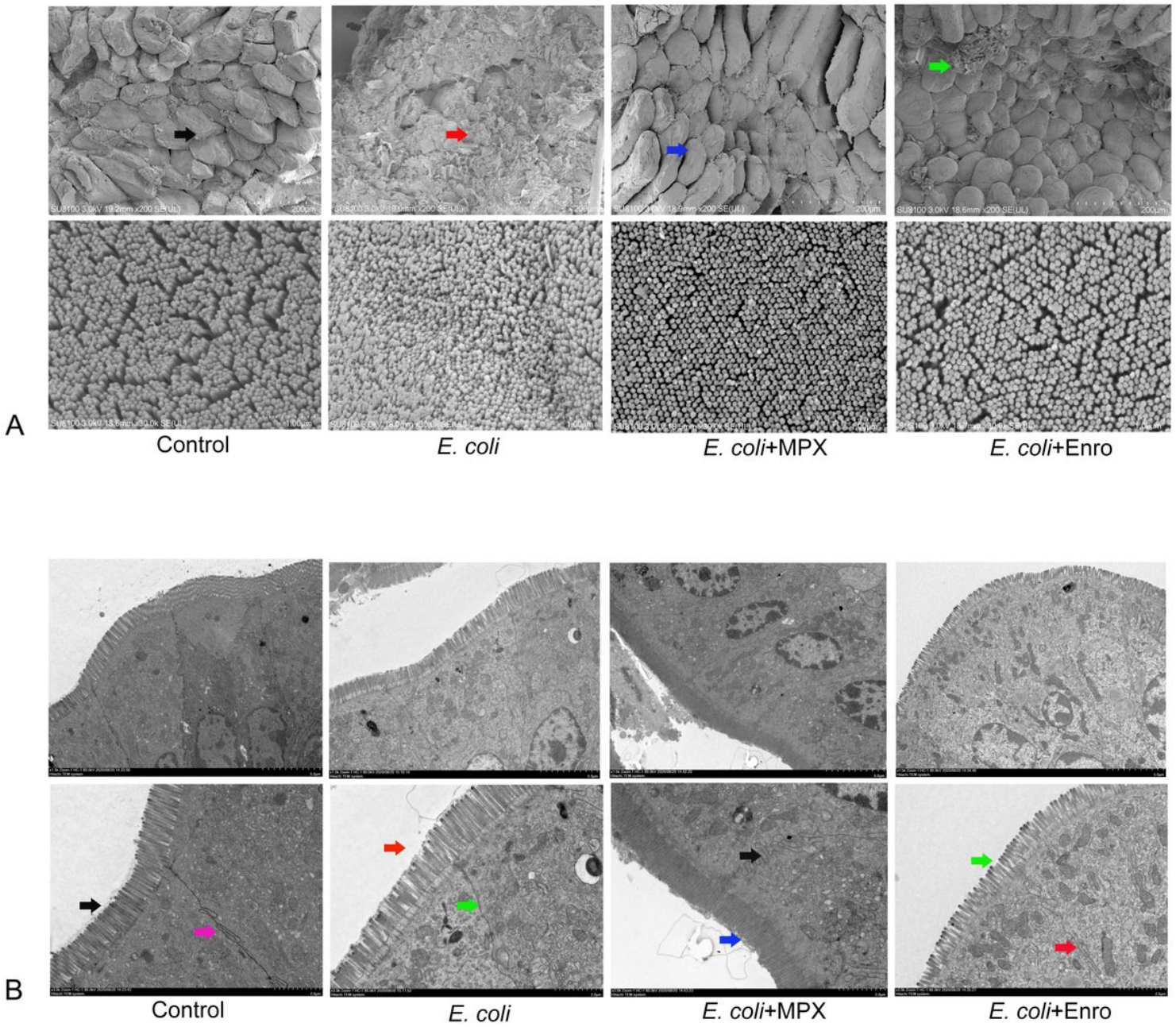

Figure 5

MPX improves the intestinal morphology of the jejunum and the microvilli of intestinal epithelial cells. (a) Morphological changes in the jejunum villi were observed by SEM (upper, 200×; lower, 30,000×); (b) Morphological changes in the microvilli and tight junction proteins in intestinal epithelial cells were observed by TEM (upper, 1500×; lower, 3000×).

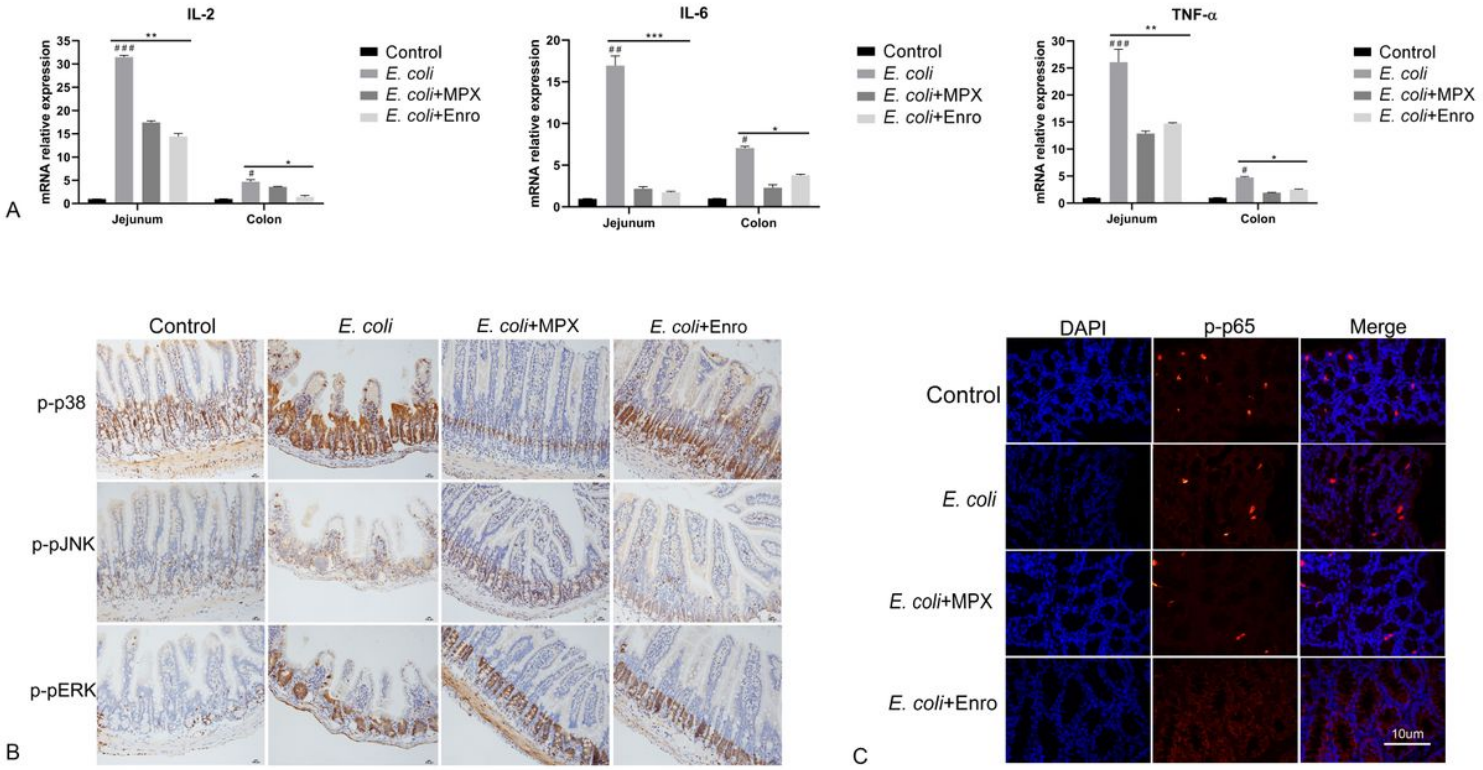

Figure 6

MPX suppresses intestinal inflammation by inhibiting the activation of the MAPK and P65 signaling pathways. (a) The mRNA expression of IL-2, IL-6, and TNF-α in the jejunum and colon after MPX treatment was measured by real-time PCR; (b) The expression of p-p38, p-pJNK and p-pERK in the jejunum after MPX treatment was determined by immunohistochemistry (bars, 100 μm); (c) The effect of MPX on the expression of p-p65 in the colon was assessed by immunofluorescence. #P < 0.05; ##P < 0.01; ###P < 0.001 E. coli vs control; *P < 0.05; **P < 0.01; ***P < 0.001 MPX and Enro treatment vs E.coli.

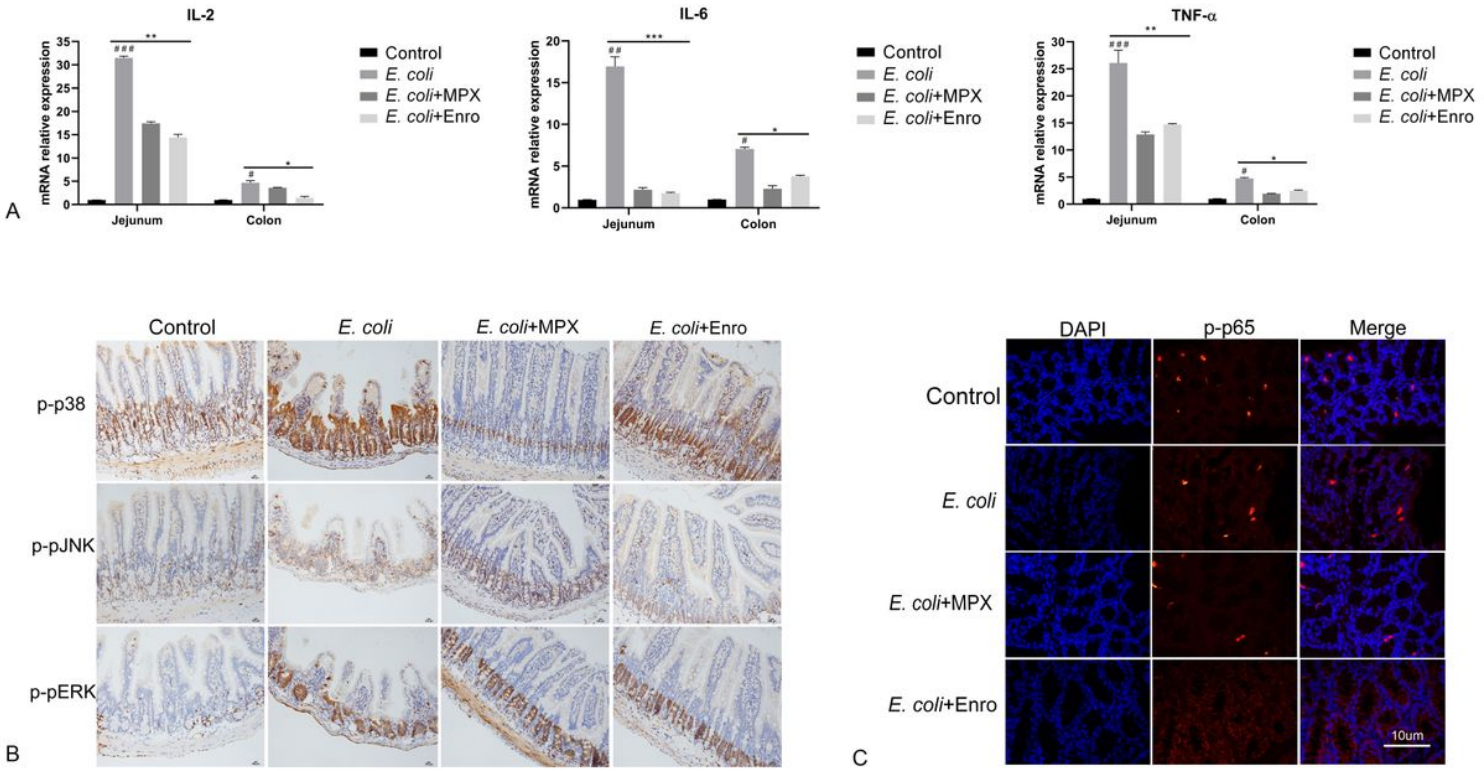

Figure 6

MPX suppresses intestinal inflammation by inhibiting the activation of the MAPK and P65 signaling pathways. (a) The mRNA expression of IL-2, IL-6, and TNF-α in the jejunum and colon after MPX treatment was measured by real-time PCR; (b) The expression of p-p38, p-pJNK and p-pERK in the jejunum after MPX treatment was determined by immunohistochemistry (bars, 100 μm); (c) The effect of MPX on the expression of p-p65 in the colon was assessed by immunofluorescence. #P < 0.05; ##P < 0.01; ###P < 0.001 E. coli vs control; *P < 0.05; **P < 0.01; ***P < 0.001 MPX and Enro treatment vs E.coli.

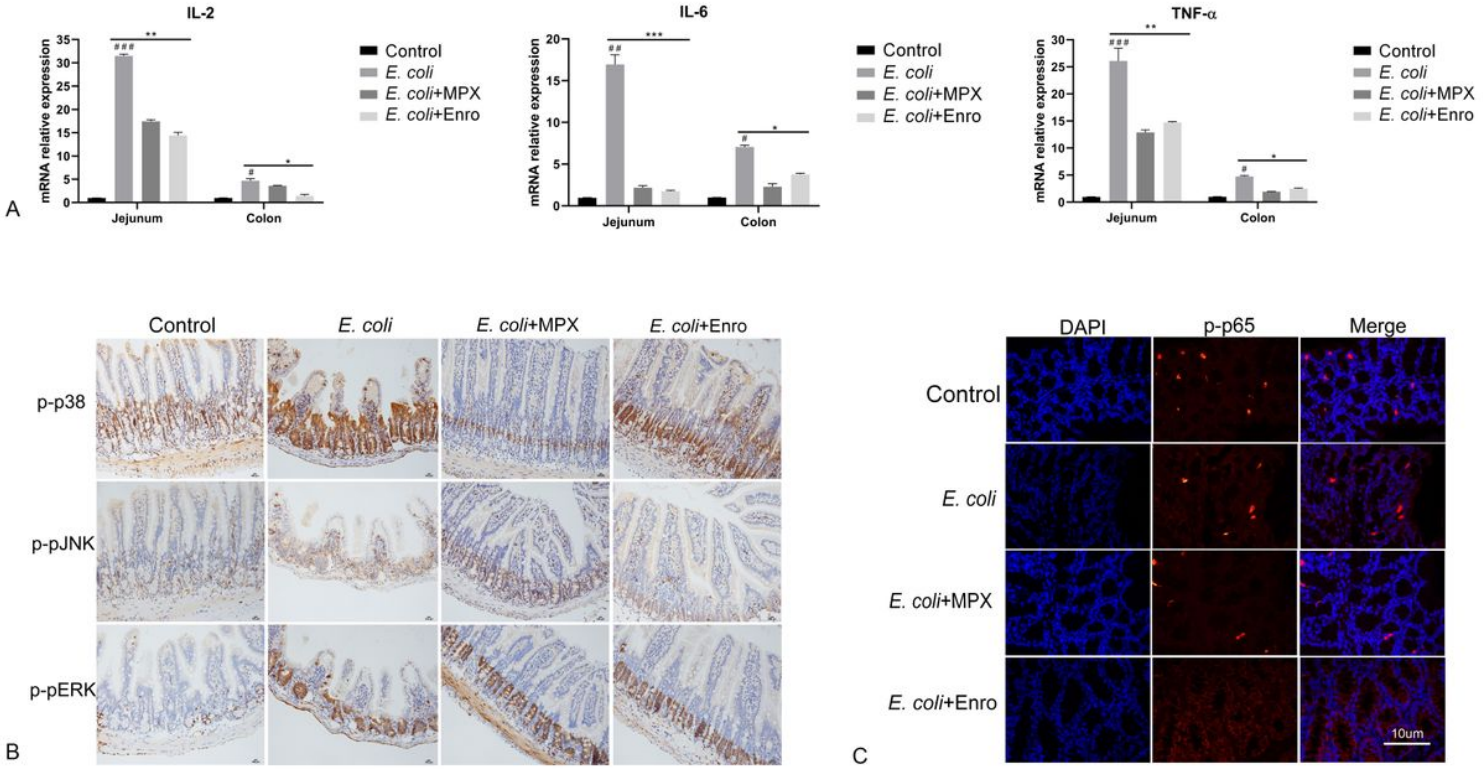

Figure 6

MPX suppresses intestinal inflammation by inhibiting the activation of the MAPK and P65 signaling pathways. (a) The mRNA expression of IL-2, IL-6, and TNF-α in the jejunum and colon after MPX treatment was measured by real-time PCR; (b) The expression of p-p38, p-pJNK and p-pERK in the jejunum after MPX treatment was determined by immunohistochemistry (bars, 100 μm); (c) The effect of MPX on the expression of p-p65 in the colon was assessed by immunofluorescence. #P < 0.05; ##P < 0.01; ###P < 0.001 E. coli vs control; *P < 0.05; **P < 0.01; ***P < 0.001 MPX and Enro treatment vs E.coli.

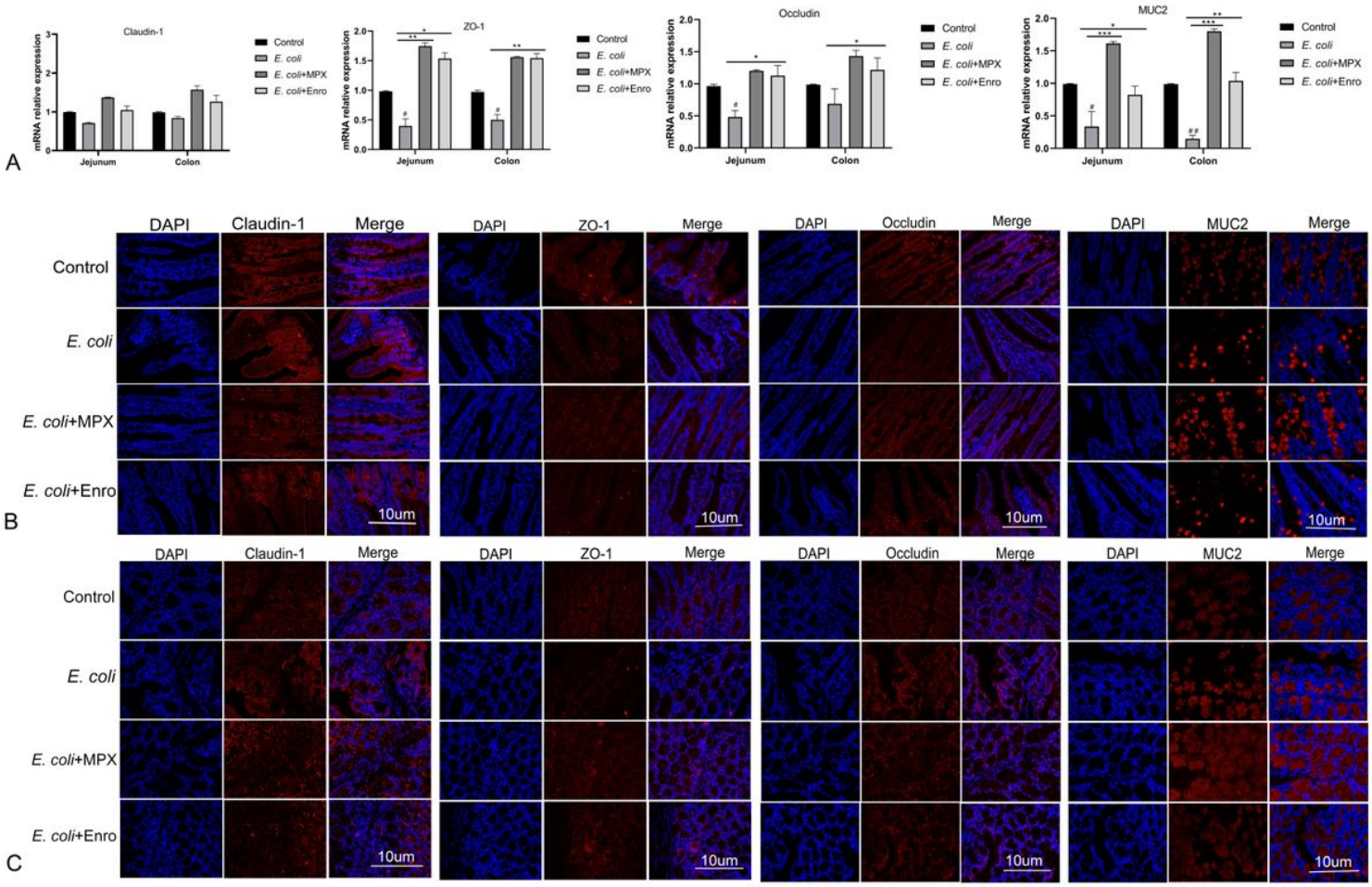

Figure 7

MPX improves the expression of tight junction proteins and mucin in the jejunum and colon. (a) The mRNA expression of claudin-1, ZO-1, occludin and MUC2 in the jejunum and colon; (b) The protein expression of claudin-1, occludin, ZO-1 and MUC2 (red) and DAPI (blue) in the jejunum; (c) The protein expression of claudin-1, occludin, ZO-1 and MUC2 (red) and DAPI (blue). Scale bar=10 μm.

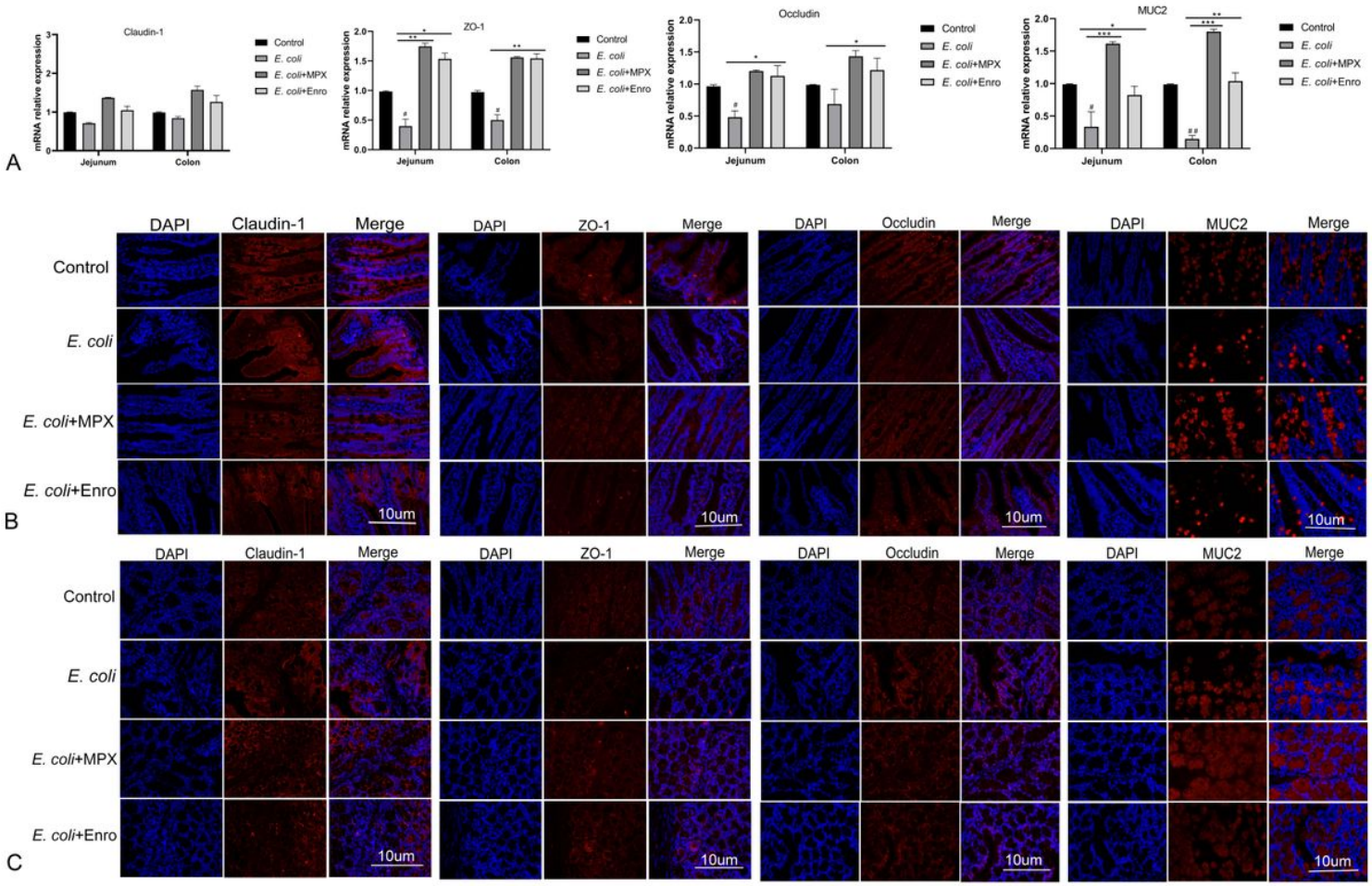

Figure 7

MPX improves the expression of tight junction proteins and mucin in the jejunum and colon. (a) The mRNA expression of claudin-1, ZO-1, occludin and MUC2 in the jejunum and colon; (b) The protein expression of claudin-1, occludin, ZO-1 and MUC2 (red) and DAPI (blue) in the jejunum; (c) The protein expression of claudin-1, occludin, ZO-1 and MUC2 (red) and DAPI (blue). Scale bar=10 μm.

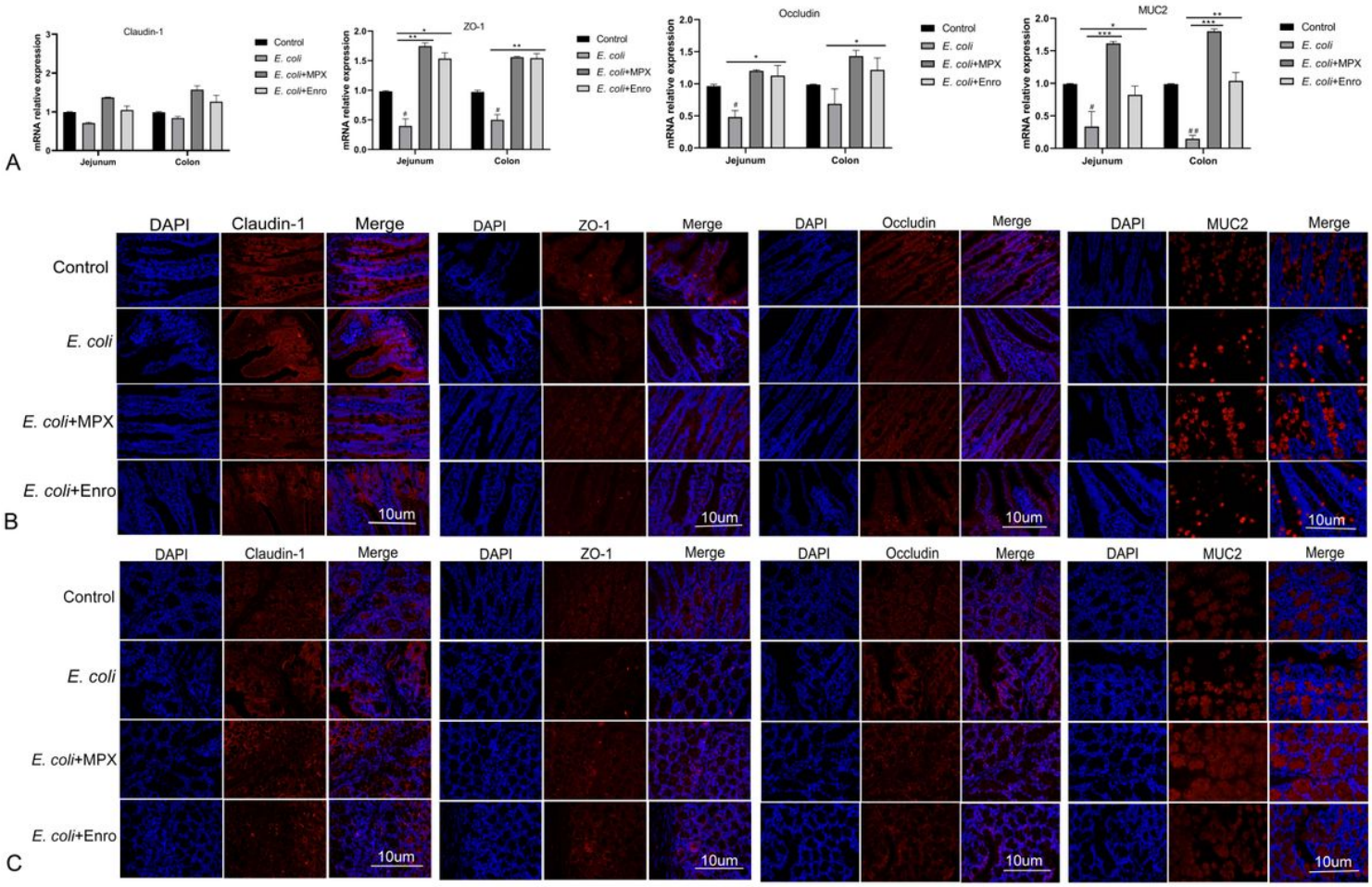

Figure 7

MPX improves the expression of tight junction proteins and mucin in the jejunum and colon. (a) The mRNA expression of claudin-1, ZO-1, occludin and MUC2 in the jejunum and colon; (b) The protein expression of claudin-1, occludin, ZO-1 and MUC2 (red) and DAPI (blue) in the jejunum; (c) The protein expression of claudin-1, occludin, ZO-1 and MUC2 (red) and DAPI (blue). Scale bar=10 μm.

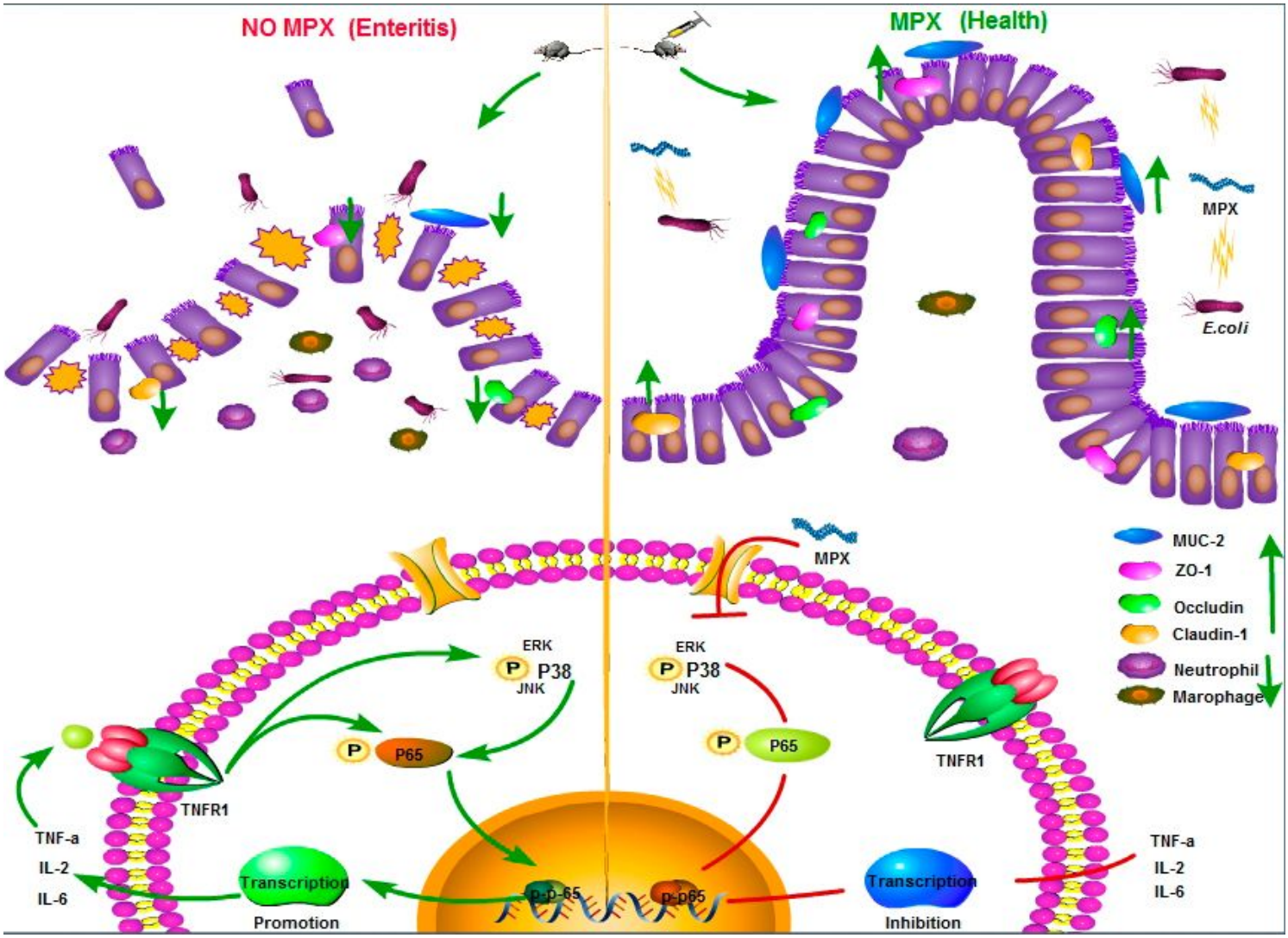

Figure 8

MPX regulates epithelial cells and in vivo signaling pathways.

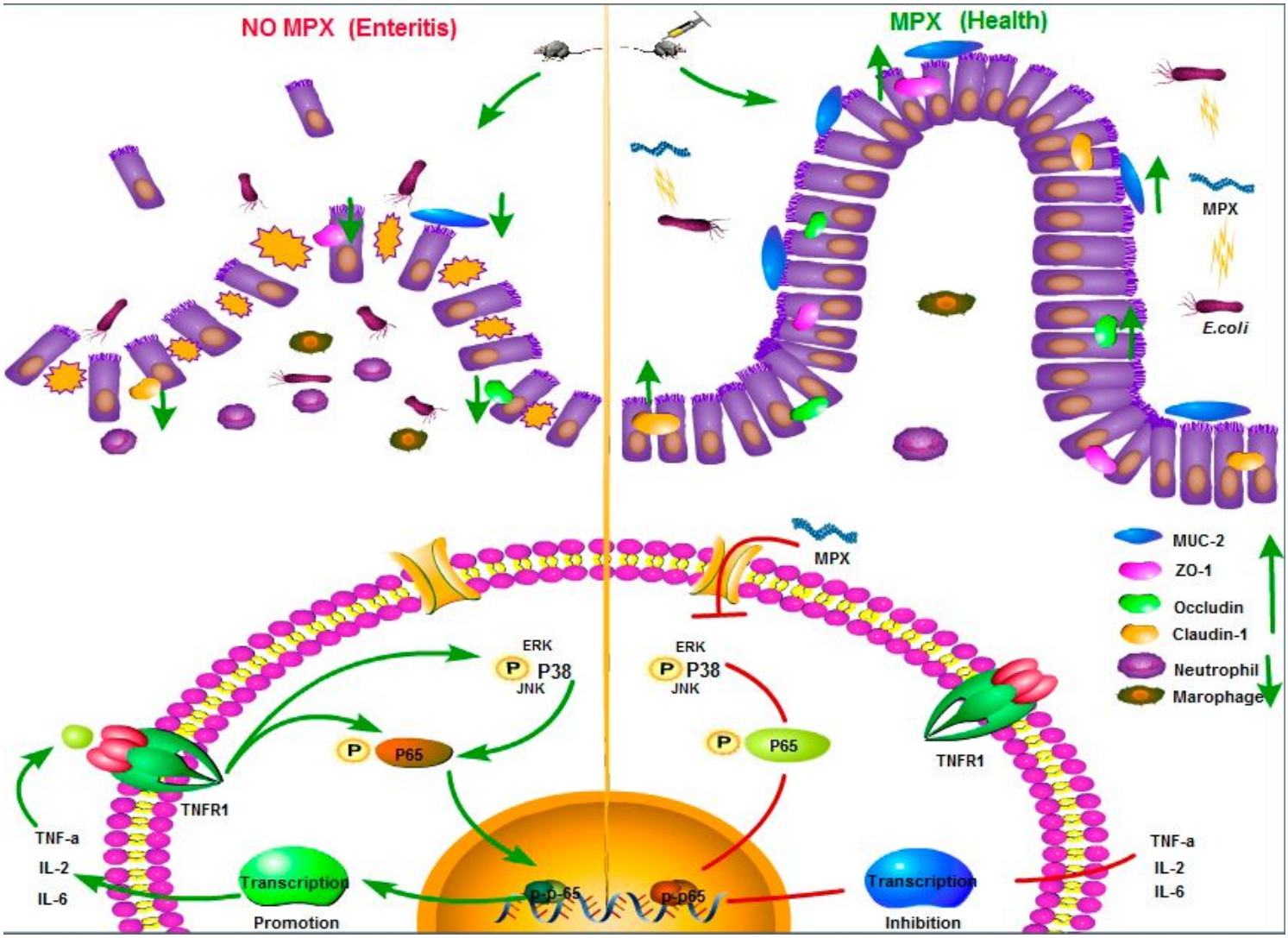

Figure 8

MPX regulates epithelial cells and in vivo signaling pathways.

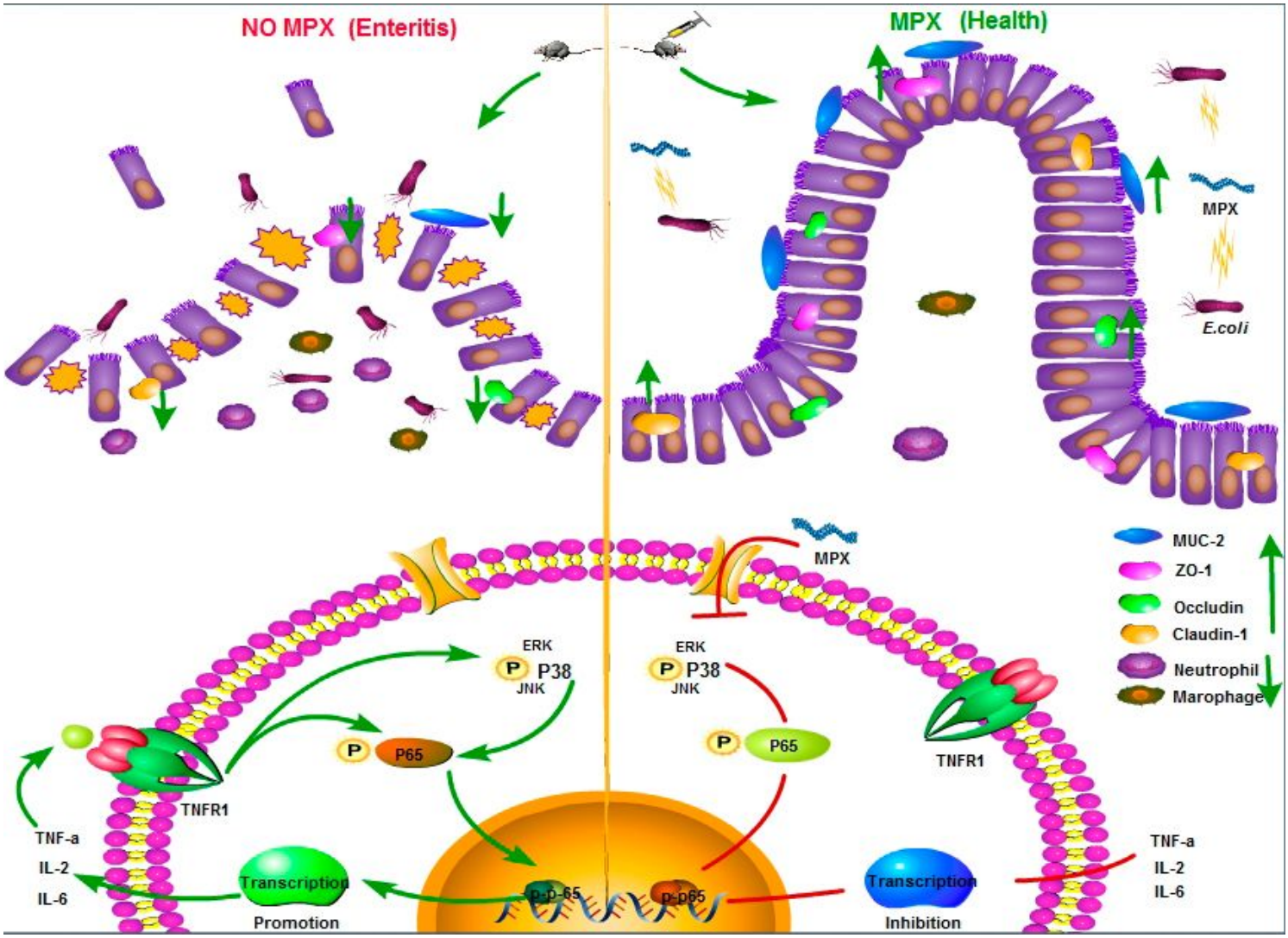

Figure 8

MPX regulates epithelial cells and in vivo signaling pathways.